Summer 2018

Effect of microstructural features on steel machinability

Mark C. Emmendorfer

Department:

EFFECT OF MICROSTRUCTURAL FEATURES ON STEEL MACHINABILITY

by

MARK CHARLES EMMENDORFER

A THESIS

Presented to the Faculty of the Graduate School of the

MISSOURI UNIVERSITY OF SCIENCE AND TECHNOLOGY

In Partial Fulfillment of the Requirements for the Degree

MASTER OF SCIENCE IN METALLURGICAL ENGINEERING

2018

Approved by

Dr. Ronald O'Malley, Advisor
Dr. Simon Lekakh
Dr. Laura Bartlett

PUBLICATION THESIS OPTION

This thesis consists of four manuscripts which two are prepared for journal articles and two are prepared for conference proceedings. Pages 29-41 is intended to be presented at Materials Science and Technology 2018 conference. The manuscript on pages 42-55 is intended for presentation at Materials Science and Technology 2018 conference. Pages 56-78 is intended for publication in the Journal of Steel Research International. The final manuscript on pages 84-96 is planned for publication in the Journal of Materials Engineering and Performance.

ABSTRACT

Non-metallic inclusions can have a tremendous impact on the machinability of steel. Some oxide inclusions such as alumina, spinel, and other refractory abrasive oxide inclusions can have a detrimental effect on machinability. Modification of oxide inclusions by calcium treatment can promote the formation of low melting point oxides such as anorthite and gehlenite inclusions that can assist in chip formation and form a lubricating layer on the rake surface of the machine tool. MnS is known to be beneficial to improving the machinability of steel. They assist in chip formation by being heavily deformed in the primary shear zone. Sulfide inclusions can also be extruded onto the rake surface of the machine tool to form a lubricating layer to resist crater wear.

Machinability tests were conducted on three grades of industrially produced steels, and on a grade produced from a laboratory heat to investigate the effect of non-metallic inclusions on the machinability of different steels.

From the results it is shown that encapsulating oxide inclusions by a sulfide shell can reduce the tool wear during machining and can assist in chip formation. The number of inclusions per unit area have a direct effect on the flank wear during machining of clean steel. Having an optimal amount of inclusions present in the steel can lead to lower flank wear. Calcium treatment can modify the oxide inclusions to be deformable during machining to assist chip formation, and stabilize the lubricating layer on the rake surface of the machine tool. The effect of grain refinement can lead to a slight improvement in the machinability of a super austenitic stainless steel with an increased amount of TiN and spinel inclusions.

ACKNOWLEDGMENTS

I would like to express my sincere gratitude and appreciation to the following people who have made guided me and supported me throughout the course of my Master's degree while attending Missouri University of Science and Technology.

I would like to thank my advisors Dr. Ronald O'Malley, Dr. Simon Lekakh, and Dr. Laura Bartlett for the tremendous help that their technical experience has assisted me these last couple years. I am extremely grateful for their continuous support throughout the course of my studies.

I would also like to thank the industrial sponsors of the Kent D. Peaslee Steel Manufacturing Research Center for supporting this research, and express my appreciation of their technical insight.

I also appreciate my fellow graduate and undergraduate students for their help on this project and many cherished memories.

Finally, I want to express my eternal gratitude for the never-ending support of my family. They have provided me with many great opportunities, and many cherished memories.

TABLE OF CONTENTS

Page

LIST OF ILLUSTRATIONS

Page

Paper II

Paper III

LIST OF TABLES

Page

1. INTRODUCTION

1.1. DEFINITION OF MACHINABILITY

The definition of machinability is the ease with which a material can be machined while maintaining a satisfactory surface finish. This can be evaluated by several parameters: tool life, tool forces, surface roughness of the workpiece, and chip formation [1]. In a recent review of machinability it was found that 85% of authors measure flank wear, while only 35% of authors measured cutting forces in their investigations [2]. The machinability of steel has been improved over the decades by modifying the non-metallic inclusions found in steel. One author summarized the improvements that have been made to improve machinability while trying to maintain good mechanical properties [3]. In the first generation of machining steels sulfur levels were elevated to increase machinability. There was limited control of MnS morphology, and oxide inclusions were controlled by removing large inclusions. In the second generation of machinable steels sulfur levels were limited to 0.1 wt%, and oxide inclusions were controlled by reducing the amount of inclusions in the steel. Third generation steels saw an increase in mechanical properties while maintaining superior machinability by modifying oxide inclusions at a regulated sulfur content. The other type of third generation steel has an elevated content of sulfur, but modification of both sulfide and oxide inclusions were achieved. Modification of these inclusions could be done by Ca-treatment to globularize the sulfide inclusions, and to modify the oxide inclusions to be malleable at machining temperatures.

1.2. MACHINABILITY TESTING

As stated before, machinability has many different factors associated with it. One of these aspects is tool life. Tool life is the measurement of machining time for a critical amount of tool wear. Machining tests in the early 1900s were completed by Taylor who constructed the Taylor equation of tool life according to Equation 1 [4].

$$V_c * T^n = C \quad (1)$$

where: V_c is cutting velocity (m/min), T is tool life (mins), coefficient n = -1/k (k is slope of line on Taylor's tool life curve, and C = constant

ISO 3685 is a machinability standard for measuring tool-life with single-point turning tools. This standard uses the Taylor tool-life equation to quantify machinability. This standard outlines many different aspects to minimize the error associated with machinability testing. It covers high-speed steel tooling, cemented carbide, and ceramic machine tools. It outlines conditions for the cutting tool, cutting fluid, and workpieces used during testing. It also outlines cutting parameters that should be used to minimize effects of the tool used. It recommends a minimum depth of cut that is twice of the tool nose radius to result in a flank wear region that can be easily resolved for measuring flank wear. It also specifies a maximum depth of cut of ten times the feed rate. The maximum feed rate is 0.8 times the tool nose radius. This standard calls for at least four machining speeds during testing, except when using ceramic tools and three speeds can be used. The testing is carried out by measuring the progressive tool wear during machining. The two major types of tool wear measured are flank wear and crater wear. The critical tool wear

values for flank wear are an average flank wear of 0.3 mm or a maximum flank wear of 0.6 mm when the flank wear region is worn irregularly. The criterion for crater wear is a function of feed rate expressed in Equation 2 [4].

$$KT = 0.06 + 0.3f \tag{2}$$

where: KT is crater depth (mm) and f is the feed rate (mm/rev)

Figure 1.1 shows the progressive flank wear curves for an example tool-life test. The red dots indicate the tool life for each of the cutting speeds chosen during the tests for a given critical tool wear value. Figure 1.2 shows the example tool-life values at the chosen cutting speeds. The secondary curve is for crater wear, which predominates at higher cutting speeds.

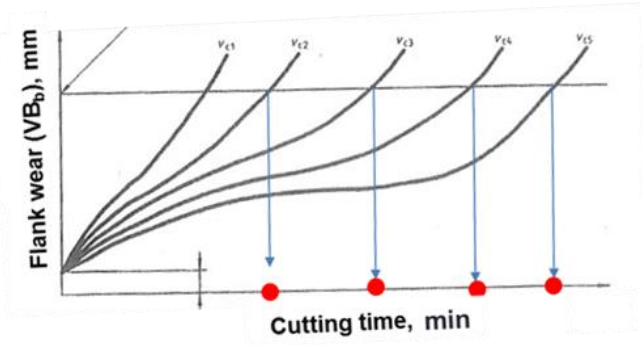

Figure 1.1: Example tool-life curves depicting the tool-life criterion [1].

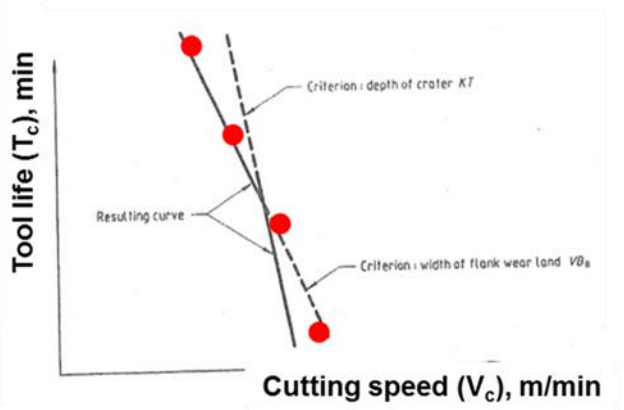

Figure 1.2: Overall tool-life curve with flank wear and crater wear criterion [1].

While the machinability standard uses the Taylor tool-life curve to quantify machinability, other authors have used an extended version of the Taylor tool-life equation. Chinchanikar et al. [5] studied the machinability of 4340 steel with varying levels of hardness, and reported their results with the extended tool-life equation with workpiece hardness shown in Equation 3 [5]. The extended tool-life equation is more complicated than the traditional tool-life equation that requires a testing matrix of machining tests to obtain tool-life data for each condition. The authors reported different tool-life equations for each material with different hardness values. It was also found that by using regression analysis that workpiece hardness has a significant impact on tool-life, and they amended the existing extended tool-life equation that accounts for feed rate and depth of cut.

$$V * T^{k_t} * f^{k_f} * d^{k_d} * H^{k_h} = C \tag{3}$$

where: V is machining speed (m/min), T is machining time (mins), f is feed rate (mm/rev), d is depth of cut (mm), H is workpiece hardness (HRC) k_t , k_f , k_h, and k_d are exponents associated with their corresponding terms.

Kuljanic et al. [6] studied difficult to machine materials, and reported his own tool life equation. His tool-life equation is much more complicated consisting of nine terms for face milling stainless steel. This equation has terms for the existing cutting parameters, stiffness of the machine system, number of inserts in the cutting tool, and interactions between various parameters. This is one example of how complicated tool-life equations can become, but as mentioned above machinability testing is a relative measurement. For instance, Bletton et al. [7] machined stainless steels with enhanced machinability by targeting anorthite oxide inclusions while using high speed steel and carbide tooling. High speed steel tools are limited to low cutting speeds, while carbide tooling can be used at high cutting speeds. The anorthite inclusions had 50% less tool wear while turning with carbide tools, but machined very similarly to the base steel when machined with high speed steel tools. This is due to the fact that anorthite inclusions can be heavily deformed and form a lubricating layer at temperatures around 800-1000°C, but this temperature is only reached when machining at higher speeds with carbide tooling.

1.3. CUTTING TEMPERATURE

It is well known that the majority of energy that goes into metal cutting is transformed into heat for a robust machine setup. The sources of the heat are generated by friction, heat generated by the chip forming process, and deformation in the shear zones [8]. It can be advantageous to measure cutting temperatures during machining to model conditions at the elevated temperatures at the chip/tool interface. Figure 1.3 shows

cutting temperatures collected by Desaigues et al. [9] while machining a high strength free-cutting steel. They observed an increase in cutting temperature as cutting speed increases. There is also a decrease in the cutting force as cutting speed increases. Chinchanikar et al. [5] reported a similar decrease in cutting forces with increasing cutting speed due to thermal softening of the workpiece. As shown in Figure 1.3 this decrease in cutting force is accompanied by an increase in cutting temperature. The heat that is generated is carried away in the chips, and can account for more than 78% of the heat removal [8].

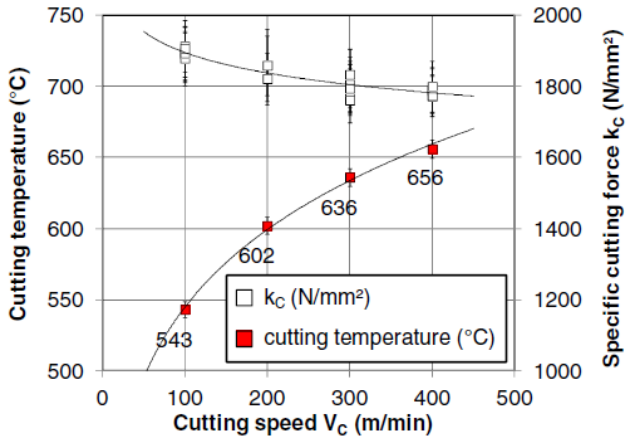

Figure 1.3: Graph showing the dependence of cutting temperature and cutting force on cutting speed [5].

Cutting temperature is also important for determining the role of inclusions during machining. MnS inclusions are known to improve machinability, but can be limited to moderate machining speeds. Oxide inclusions can be beneficial for machinability depending of the temperature encountered at the chip and tool interface. Bletton et al [7]

studied malleable oxides in machining of 316L stainless steel. They found that anorthite, a low melting point oxide phase, could be greatly deformed in the primary shear zone during machining. This was due to the cutting temperature (800-1000°C), and the oxides being deformable at this temperature. Fang and Zhang [10] machined a Ca-S treated stainless steel and a conventional stainless steel and found the Ca-S steel had a superior machinability. They concluded the improvement of machinability was due to the anorthite and MnS inclusions that adhered to the rake surface of the machine tool. They found that the anorthite oxide inclusions were closer to the cutting edge of the tool, and the MnS layer was further away from the cutting edge. This could be due to the improved stability of the oxide lubricating layer at higher temperatures. Desaigues et al. [9] measured temperatures across the width of the machine tool and found temperature decreases as a function of distance from the cutting edge. One study reported a cutting temperature of 1150°C while machining a Ca-S stainless steel and the ability of gehlenite oxide inclusions to adhere to the rake surface of the tool reducing both flank wear and crater wear [11].

1.4. CHIP FORMATION

Chip formation is a fundamental part of the metalcutting process. When the machine tool comes into contact with the workpiece a large amount of energy is introduced to the workpiece to form a chip. This energy involves shearing of the workpiece material, and the newly formed chip undergoes large amounts of plastic deformation as it passes over the machine tool [12]. Machine chips can take many forms: continuous, segmented, and discontinuous chips just to name a few types. Ductile materials will usually have a continuous chip which occurs due to the chips not fracturing

in the shear plane [12]. Mastsumoto et al. [13] reported that chip segmentation occurs during instability of the cutting process. This is the result of periods of the chip undergoing large amounts of strain and momentarily adhering to the rake surface of the tool.

The machine chip can be described in having multiple regions that can be seen in Figure 1.4. This is an optical micrograph of a chip root obtained during a quick stop experiment [14]. The quick stop experiment is extremely useful in capturing the moment of chip formation. This is accomplished by rigging the machine tool to separate from the workpiece at a high rate of speed in the same direction of the rotating workpiece. This will successfully have the machine chip still adhered to the workpiece, which will then be mounted and polished to examine chip formation. In Figure 1.4 there are two important regions of the machine chip. The primary shear zone and the secondary shear zone or flow zone. Shelbourn et al. [14] machined a medium carbon steel and characterized the shear zones in the machine chips. The primary shear zone is outline by the red dashed lines. The flow zone of the machine chip is located at the rake surface/chip interface. The flow zone undergoes tremendous amounts of plastic deformation. They reported that the pearlite structure was similar to those found in wire drawing operations. On the other hand, in the flow zone there was equiaxed cells of ferrite. Wright and Robinson [15] studied the flow zone when machining copper and found that this region experienced higher strain rates and temperatures compared to the primary shear zone. It can be seen in Figure 1.4 that the microstructure cannot be resolved optically because of the large amounts of plastic deformation. The influence of non-metallic inclusions in the primary shear zone and flow zone will be discussed later.

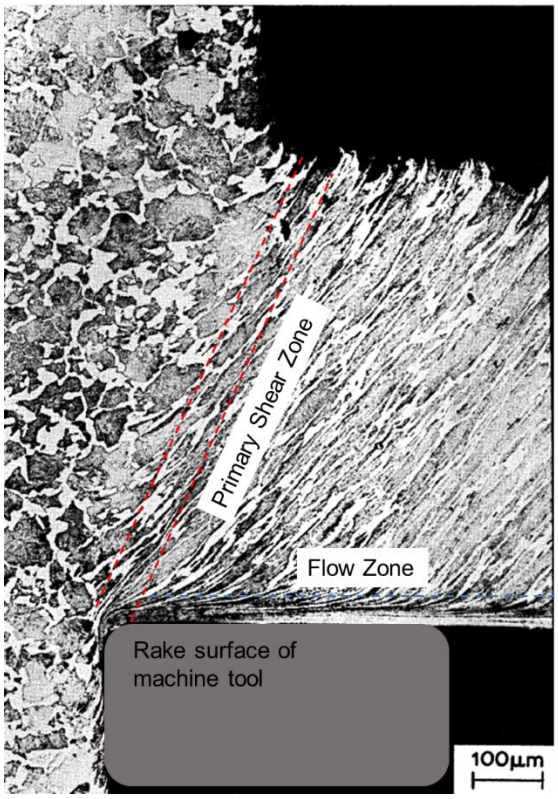

Figure 1.4: Machine chip collected during a quick-stop experiment showing the different deformation zones [15].

1.5. TOOL WEAR

There are many different types of tool wear that can occur during machining. Measuring tool wear is an essential part of tool-life testing. The most common forms of tool wear to be measured during testing are flank wear and crater wear [16]. Examples of flank wear and crater wear (rake face) can be seen in Figure 1.5. Flank wear occurs on the major cutting edge of machine tool, and it commonly measured for tool-life criterion. The length of the flank wear is associated with the depth of cut used during the machining process. Crater wear occurs on the rake surface of the machine tool. The rake

surface is the surface that the machine chip passes over during machining and crater wear will occur in this region.

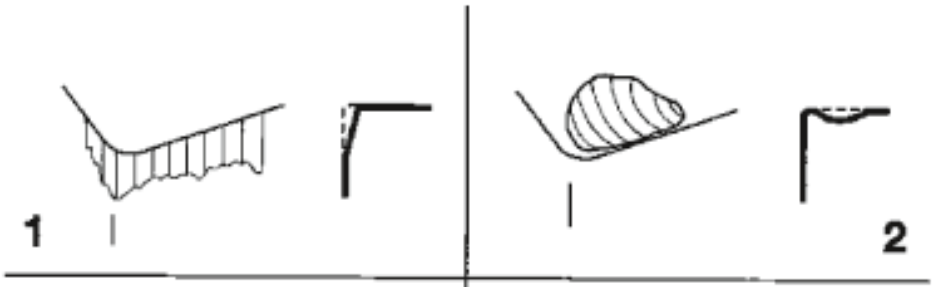

Figure 1.5: Schematic showing examples of flank wear (1) and crater wear (2) [16].

Sources of tool wear include adhesion, abrasion, and diffusion wear. Adhesive wear occurs at low cutting speeds due to the adhesion of workpiece material to the machine tool. The formation of built-up edge is associated with adhesive wear [12]. Abrasive wear occurs over a broad range of cutting speeds and is associated with abrasive particles that occur in the steel [1]. These can be in forms of oxide, nitride, and carbide inclusions and precipitates. Diffusion wear occurs at higher cutting speeds due to the higher cutting temperature. The diffusion wear occurs on the rake surface of the machine tool. During machining of steel iron can diffuse into the cobalt matrix of the cemented carbide tool, and cobalt can diffuse into the machine chip. There will also be some dissolution of the tungsten carbides to form mixed carbides with the diffused iron in the machine tool [1]. These mixed carbides have lower hardness compared to the pure tungsten carbide phase. These mixed carbides can then be worn away causing abrasive wear on the rake face known as crater wear.

1.6. INFLUENCE OF NON-METALLIC INCLUSIONS ON THE MACHINABILITY OF STEEL

Non-metallic inclusions commonly found in steel can be classified as sulfides and oxides. Non-metallic inclusions can have multiple influences on machinability. Oxide inclusions have been linked to cause abrasive wear during machining [17]. Ca-treatment is commonly employed to modify oxide inclusions for better castability during casting to avoid nozzle clogging. This also can affect the machinability of the steel. Diggs et al. [18] reported enhanced machinability of stainless steel by Ca-treatment of oxide inclusions targeting anorthite and gehlenite regions of the $CaO\text{-}SiO_2\text{-}Al_2O_3$ ternary phase diagram. There are multiple factors that sulfide and oxide inclusions have on the machinability of steel: effect on general steel machinability, behavior during machining, and the possibility to form a lubricating layer are discussed.

1.6.1. General Effect of Inclusions on Steel Machinability. It is well known that oxide inclusions such as alumina or spinel type inclusions contribute to abrasive wear of the cutting tool during machining. Hard inclusions that do not deform at machining temperatures have a detrimental effect on machinability [9]. These inclusions come into contact with the machine tool and cause abrasion wear. Faulring et al. [17] evaluated the machinability of air-melted and vacuum melted steels to investigate the effect of different oxide inclusions on machinability. They found that the high temperature oxides such as mullite or alumina lead to higher flank wear rates. This is due to the high temperature hardness of these phases. They also reported that a steel with glassy inclusions had a much lower flank wear than a steel with mullite inclusions present, even though both types of inclusions were similar in size and shape. Unmodified

oxide inclusions and other abrasive inclusions with a high hardness can be detrimental to tool life by causing abrasive wear.

Modified oxide inclusions can actually be beneficial for the machinability of steel. Modification is commonly done in the form of Ca-treatment. Hamann et al. [19] found that Ca-treatment can reduce the cutting forces measured during machining of a treated steel compared to a conventional steel, which also had a better machinability. Fang and Zhang [10] reported a lower tool wear when machining a Ca-S treated steel resulting from the lower abrasive nature of the Ca-containing oxide inclusions compared to the Al_2O_3 inclusions in the conventional steel. Complex Ca-containing oxide inclusions were also reported to be softer than SiO_2 type oxides [20]. Modified oxide inclusions that are beneficial for machinability for Si and Al-killed heats are anorthite and gehlenite, and for Si and Mn-killed heats the spessartite oxide inclusions are targeted for enhanced machinability [3]. Another method to decrease the abrasiveness of oxide inclusions is by enveloping them with a sulfide shell. Previous researchers [3,21] reported better machinability for steels that had Ca-Al oxide inclusions with sulfide shells.

Sulfur is added to steel to combine with manganese to form MnS inclusions which can improve machinability. Jiang et al. [22] investigated the effects of composition, morphology, and area fraction of sulfide inclusions on the machinability of a resulfurized steel. They measured cutting forces for different cutting conditions and found that the cutting force decreases when machining elongated sulfide inclusions. They also noted an increase in cutting force when machining a steel with a larger interspacing between sulfide inclusions. One of the steels tested was Ca-treated, and the globularization of the sulfide inclusions led to a decrease in flank wear. Yaguchi [23] studied the effect of MnS

inclusions on the formation of built-up edge. The phenomenon of built-up edge occurs when workpiece material adheres to the machine tool causing increased tool wear and can impair the surface quality of the machined surface. His results show that sulfur additions shift built-up edge to higher cutting speeds. Built-up edge can also be reduced by a larger MnS inclusion size.

Behavior of Inclusions During Machining. Some non-metallic inclusions can be considered non-deformable inclusions. When hard inclusions are present in the primary shear zone they will fracture instead of undergoing deformation. This leads to microcracks that are initiated by internal particle failure [24]. Alumina inclusions will initiate cavities at the matrix interface and remain undeformed [25]. Zanatta et al. [26] machined VP100 mold steel with different amounts of Ti(C,N) inclusions present in the steel. They reported lower cutting forces with a steel with large Ti(C,N) inclusions which could be due to the fracturing of these inclusions during machining. However, the elevated Ti content in the steels resulted in a lower volume of material removed compared to the base steel for an equivalent tool life. These hard inclusions are less effective in chip breaking compared to deformable inclusions.

Another type of inclusion has the ability to be deformable during machining. Ca-treatment of oxide inclusions modifies the composition of harmful oxides into low melting point oxide inclusions that can be deformable at machining temperatures. Kiessling [25] notes that the complex Ca-Al-silicates can be heavily deformed during machining. Bletton [7] studied different oxide inclusions in machining of stainless steel also reported the ability to heavily deform anorthite oxide inclusions. This is due to them being malleable at temperatures encountered at the tool-chip interface allowing them to

deform into fine elongated inclusions in the primary and secondary shear zone. These inclusions act as an internal lubricant to allow for easier chip formation and breakage during machining. The Ca-Al oxides enveloped by sulfide inclusions also have the ability to be deformed during machining.

MnS are very beneficial to chip formation due to being easily deformed in the primary and secondary shear zone. Deformable inclusions like MnS and the oxides mentioned above act as stress raisers in the shear zones and help facilitate chip formation. When plastic deformation occurs in the shear zones, voids form at the inclusion/matrix interface as more deformation occurs the inclusions elongate in the direction of shear providing easier propagation of cracks to assist chip breaking [9,24,25,27]. Liu and Chen [28] studied the effect of MnS morphology on chip formation. They reported that globular MnS inclusions are more beneficial for chip formation because voids formed around the inclusions cannot be rewelded during deformation. This may occur if the MnS inclusions are heavily deformed and form thin elongated inclusions during machining, the voids would be thinner and could close under the high compressive stresses in the primary shear zone. The inclusions that have the ability to deform during machining are more effective for chip formation.

1.6.2. Lubricating Layer Formation. Many studies report that the formation of a lubricating layer on the rake surface of the machine tool has a huge impact on obtaining longer tool lives at higher machining speeds. This is due to the fact that the formation of a lubricating layer can minimize crater wear, because the lubricating layer can inhibit diffusion of workpiece material into the machine tool. The formation of the lubricating

layer is a complex process that requires certain conditions on the machine tool in order for a stable layer to exist.

Helle [29] thermodynamically simulated and experimentally verified the conditions that are necessary to form a lubricating layer on a cemented carbide tool. In the beginning of his experiments it was unknown why lubricating layers could not form on an uncoated carbide tool. It was found that oxidation of the tool surface or presence of suitable oxide inclusions present in the steel are essential for layer formation. Even the formation of a stable sulfide layer requires the presence of oxide inclusions. The oxidation of the TiC on the surface of the cutting tool is the first step to produce the foundation of the lubricating layer. A thin layer of titanium oxide can form from the TiC coating by being oxidized by less stable oxide inclusions like: MnO or a reaction involving MnS and CaO, that other oxide inclusions can adhere to if the oxide inclusions are capable of bonding to this layer. Once the tool surface is oxidized inclusions present in the steel are extruded onto the rake surface of the tool. This continuous build-up of inclusions forms the lubricating layer on the cutting tool. Inclusions with good deformability is not necessary for layer formation. When inclusions become too elongated they lose their ability to form a stable lubricating layer. He also found that machining speed, thus cutting temperature, is important for a stable lubricating layer. As cutting speed increases MnS inclusions become less stable because of their increased plasticity at the higher cutting temperatures and the layer will gradually disappear. Therefore, oxide lubricating layers are more stable at higher cutting speeds. However, the oxide layers also have cutting speed limitations due to the possibility of increased plasticity. Qi et al. [11] reported a similar hypothesis on lubricating layer formation. The inclusions are plastically deformed during machining and are

extruded onto the rake surface of the tool. The inclusions will then adhere to the surface of the tool if there is a strong affinity to bond to the TiC coating. Next, the tool temperature decreases due to the presence of the lubricating layer separating the tool from the heat of friction, this allows the lubricating layer to harden and stabilize. Lastly, more inclusions are extruded onto the existing layer and a stable layer is formed.

The lubricating layer has multiple impacts on improving the machinability of steel. Akasawa et al. [30] conducted machinability studies on free-machining stainless steels and found evidence of S, Bi, Ca, and Cu on the cutting tool surface which could be linked to the formation of a lubricating layer. Bittes et al. [31] reported that an increased Ca content in (Ca,Mn)S could improve the stability of the lubricating layer, but mentioned that pure CaS inclusions have a higher hardness that can led to an undesirable impact on machinability. The formation of a lubricating layer while machining a Ca-treated steel led to a decrease in adhered workpiece material during machining [32]. Tönshoff et al. [33] reported a decrease in flank wear and crater wear due to a lubricating layer formation. They also observed that at higher cutting speeds the lubricating layer has enhanced plasticity and disappeared after machining for a short time. Matsui et al. [34] investigated the behavior of the lubricating layer while sequential machining of a Ca-treated steel and a Ca/Mg-added steel. First, they machined the Ca/Mg treated steel that resulted in some crater wear, then machined the Ca-treated steel and saw the formation of the lubricating layer. In the other experiment, they machined the Ca-treated steel, formed a lubricating layer, then machined the Ca/Mg treated steel and reported an increase in crater wear. The results of these experiments are shown in Figure 1.6. It is interesting to notice that in the first experiment the rapid progression of tool wear, and it plateaus while

machining the Ca-treated steel since the formation of the lubricating layer resisted the progression of crater wear. On the other hand, when the Ca-treated steel was machined first, the lubricating layer quickly disappeared when machining the Ca/Mg treated steel due to the abrasive oxides present in steel.

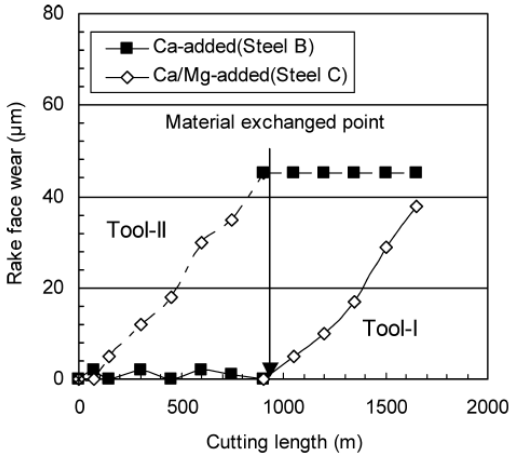

Figure 1.6: Evidence of the ability of a lubricating layer to resist crater (rake) wear [34].

1.7. CLEAN STEEL MACHINABILITY

Steel cleanliness is a measure of the low content of impurities present in the steel. This can also be a measure of a low non-metallic inclusion content within the steel. Clean steels are associated with great mechanical properties, but this cleanliness has a detrimental effect on machinability [35]. Ånmark et al. [36] reported a decrease in machinability for a clean steel compared to a reference steel with a higher sulfur level. He concluded when machining these steels a lack of lubricating layer could persist. This would lead to a rapid increase in crater wear and workpiece adhesion onto the machine

tool. Since a stable lubricating layer requires a steady extrusion of inclusions to be deposited onto the tool the lack of these inclusions in the clean steel could result in no lubricating layer forming. In another study Ånmark et al. [37] suggested that without a lubricating layer the friction between the workpiece and cutting tool would increase resulting in a higher cutting temperature and higher tool wear. Liu and Chen [28] studied the effect of total oxygen on the machinability of a free cutting steel. They measured the total oxygen of multiple samples, and found that the lowest flank wear resulted at an intermediate total oxygen level. The lowest total oxygen had a higher flank wear, and when the total oxygen was increased from 0.0105 to 0.0150 a rapid increase in tool wear was observed. At the intermdiate oxygen content, the improved machinability was due to a globurization of the MnS inclusions. The poor machinability at the higher oxygen contents was due to abrasive oxide and oxy-sulfide inclusions present in the steel.

1.8. EFFECT OF GRAIN SIZE ON MACHINABILITY

The effect of grain size on machinability is not a topic that is covered extensively. Jiang et al. [38] investigated the effect of austenite grain size on tool life while machining 304L stainless steel. Samples were hot worked to reduce the austenite grain size, then heat treated at different holding temperatures to influence growth of the austenite grains, and then water quenched. Metallography showed an increase in grain size as the holding temperature increased. Machining tests were done on each of the samples and the results can be seen in Figure 1.7. From these results it is evident that as grain size increases machinability decreases. Jiang concluded that the lower tool life of the hot-forged sample was due to an inhomogeneous distribution of grain size, and the machine tool failed due to chip breakage instead of the normal flank wear criterion of the other specimens.

Hoseiny et al. [39] reported similar results in milling P20 mold steel. That experiment measured the martensite packet size, and found that as prior austenite grain size increases the martensite packet size increases as well. They reported an increase in tool life for specimens with a smaller martensite packet size. Komatsu et al. [40] studied the effect of crystal size during mircomilling of stainless steel. He reported a reduction in the tendency for burr formation while machining the finer grain stainless steel. This resulted in an increase in surface finish that is necessary during the micromilling process.

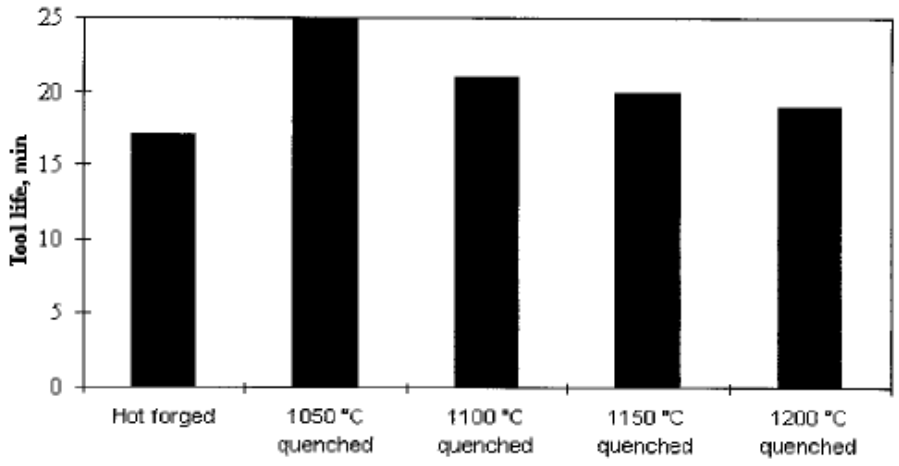

Figure 1.7: Tool-life results of hot forged bars held at different holding temperatures [38].

1.9. STATEMENT OF PURPOSE

The goal of this research was to investigate the effects of non-metallic inclusions and steel microstructure on steel machinability. This research is divided into four parts. Part one investigates different fine grain practices of AISI 4140 steel, and how it affects the inclusion populations and how it is related to machinability. The ability to modify oxide inclusions to attain longer tool life is discussed. Part two outlines the effect of steel

cleanliness on machinability of AR450 abrasion resistant steel. The influence of inclusions for improved machinability are also discussed. Part three deals with the effect of Ca-treatment on the machinability of 303 stainless steel. The multiple influences of Ca-treatment for improved tool life is reported. Part 4 investigates the effect of grain size on the machinability of super austenitic stainless steel. The material studied in these investigations were produced in industrial facilities, and the machinability tests were conducted in the laboratory.

2. METHODOLOGY

2.1. MATERIAL CHARACTERIZATION

The following sections detail the methods used for analyzing the materials studied.

2.1.1. Metallography and Non-metallic Inclusion Analysis. Samples for metallography and non-metallic inclusion analysis were taken in the transverse (T) and longitudinal (L) directions from the material used for the machining tests. Multiple samples were taken in both directions to characterize the microstructure and non-metallic inclusions present in the machining volume of the specimens. Samples were mounted in bakelite, and polished to 0.1 μm finish for scanning electron microscope (SEM) analysis equipped with energy dispersive spectroscopy (EDX) to characterize the non-metallic inclusions in the steel.

Non-metallic inclusions were analyzed using an ASPEX 1020 SEM/EDX. An automated feature analysis (AFA) was used to count 2000 inclusions in an area of 4-25 mm^2. An additional analysis was run to classify oxide inclusions in the steel by analyzing a large area of 25-30 mm^2 which are less numerous than the sulfide inclusions in the studied steels. The data collected from the analysis was analyzed using methods previously detailed by Harris et al. [41].

2.1.2. Hardness Measurements. Hardness profiles were taken of the cross section of the machining specimens to verify consistency of the steel structure throughout the machining volume. Hardness measurements were taken every 0.125” and Rockwell Hardness C-scale (HRC) was used during testing.

2.1.3. Machine Chips Analysis. Machine chips were collected at each of the cutting speeds to observe the behavior of inclusions during machining. The machine chips were mounted, polished, and examined used a SEM/EDX to look at the cross-section to observe the behavior of inclusions in the primary shear zone and flow zone of the machine chips. The thickness of the machine chips was measured to calculate the shear angle using Equation 3 [39]:

$$\tan\varphi = \frac{t}{T}\cos\alpha \div (1 - \frac{t}{T}\sin\alpha) \quad (2)$$

where: φ is shear angle, t is uncut chip thickness (feed rate), T is measured chip thickness, and α is rake angle of cutting tool. A Dorian tool holder MSRNL 12-4B with a rake angle of -7° determined the rake angle for the machining tests.

2.1.4. Post-Machining Tool Analysis. The rake surface of the machine tool was analyzed in a SEM/EDX to observe the formation of a lubricating layer formed during machining. The flank wear surface of the machine tool was analyzed to verify the final flank wear of each test.

2.2. MACHINABILITY TESTING METHOD

The following sections detail the methods using for machinability testing.

2.2.1. General Method. The turning tests were carried out on a HAAS TL-1 CNC lathe. The machinability of the studied materials was quantified by measuring the progressive flank wear during machining. Flank wear was measured with a DinoLite AM 4815ZTL digital microscope. Tool-life is the amount of machining time for a critical value of flank wear. The critical value of tool wear is dependent on the material being machined. The surface layer of the workpiece was removed prior to starting the

machining tests, and a new machine tool was put in the tool holder for the machinability tests.

2.2.2. Tool-life Testing of 4140 Steel (Part I). The machinability of AISI 4140 steel was quantified by measuring the progressive flank wear during machining until the tool-life criterion was satisfied. The machining parameters for this study are as follows: 460, 655, and 850 SFM (ft/min) to obtain tool life curves with constant 0.005" ipr (inch/rev) feed rate, 0.062" depth of cut, and dry cutting condition. Experimental Taylor tool-life curves were calculated from the tool life data. A flank wear value of 0.15 mm was used as the tool-life criterion for this study. The workpiece has a diameter of 3.5 inches, and a machining length of 8.75 inches. A Sandvik Coromant SNMG 432-PM 4325, a *Ti(C,N)+ Al_2O_3* and *TiN* coated cemented carbide tool was used for the machining tests.

2.2.3. Fixed Volume Machining Test for AR450 Steel (Part II). The machinability of AR450 abrasion resistant steel was measured by single point turning of a fixed volume of material for each test. Twenty machining passes were completed during each test. The cutting parameters were: 0.012" ipr (in/rev) feed rate, 0.03" depth of cut, 270 SFM (ft/min) cutting speed, and coolant were used for the machining tests. Duplicate tests were performed for each specimen to assess the repeatability of the results. A cemented coated carbide cutting tool SNMG 431-QM 4325 manufactured by Sandvik Coromant was used.

2.2.4. Tool-life Testing of 303 Stainless Steel (Part III). Tool-life testing was conducted to quantify the machinability of resulfurized 303 stainless steel (SS). Progressive flank wear was measured during the machining tests, and a flank wear value

of 0.07 mm was used as the tool life criterion. The cutting parameters used were: 655 SFM (ft/min) machining speed, 0.062” depth of cut, 0.008 ipr (inch/rev) feed rate, and dry cutting condition. A Sandvik Coromant SNMG 432-MM 1125 coated cemented carbide insert was used.

2.2.5. Fixed Volume Machining Test of Super Austenitic SS (Part IV). Fixed volume machining tests were carried out to measure the progressive flank wear during machining. The cutting parameters chosen for this study: 175 SFM (ft/min) machining speed, 0.032” depth of cut, 0.005 ipr (in/rev) feed rate, and dry cutting condition. Two fixed volume machining tests were completed for each condition to test the repeatability of the machining conditions. The test was completed after machining 19 in^3 of material. A Sandvik Coromant SNMG 431 QM-235 coated cemented carbide tool was used for this study.

3. SUMMARY OF PAPERS

Paper I: Effect of Aluminum and Vanadium Fine Grain Practice on the Machinability of 4140 Steel

Paper 1 investigated the effect of different fine grain practices on the inclusion population and machinability of two different steels. A vanadium fine grain practice steel (G1) was compared to an aluminum fine practice steel (G2). Experimental Taylor curves were constructed from tool-life data collected from machining tests. It was found that specimen G2 had a better machinability at all the tested cutting speeds.

The main impact of the better machining properties of G2 was related to the non-metallic inclusions. Al-rich oxide cores were enveloped in MnS inclusions, and a sulfide shell was observed surrounding the Ca-Al oxide inclusions. The abrasive nature of the oxide inclusions could have been reduced by being surrounded by a sulfide shell. This could be linked to the longer tool life observed for G2. The enveloped oxide inclusions were able to be deformed during machining which could have assisted chip formation.

Paper II: An Investigation of the Machinability of Abrasion Resistant AR450 Steel

Paper 2 studied the effects of steel cleanliness on the machinability of AR450 steel produced under different conditions. One of the steels was produced under steady state casting condition (S2), while another was cast under non-steady state (S3). One of the steels was cast under similar conditions (S4) of specimen S2 to compare the repeatability of the experimental results. Specimen S5 was produced using the BOF steelmaking process, whereas all the other steels were produced with the EAF steelmaking process. Non-metallic inclusions were classified with a SEM/EDX. The

machinability of the four industrially produced steels was compared by conducting fixed volume machining tests.

The results show that the tool wear is dependent on the inclusion content of the steel. At a low value of inclusions per unit area, or clean steel, flank wear was increased due to poor chip breakability due to lack of inclusions. At high values of inclusions per unit area the flank wear rapidly increased due to a large volume fraction of abrasive inclusions. However, at intermediate values of inclusions per unit area the flank wear was minimized. This shows that an optimal amount of inclusions per unit area may be necessary for chip formation and result in less flank wear.

Paper III: Modification of Inclusions to Enhance the Machinability of Resulfurized 303 Stainless Steel

Paper 3 deals with the effect of Ca-treatment on the machinability of resulfurized austenitic stainless steel. Three grades of industrially produced 303 stainless steel, one base (N1) and two Ca-treated grades (N2, N3) were studied to compare the machinability of these steels. Non-metallic inclusions were characterized using a SEM/EDX. Progressive flank wear was measured during testing. An increase of five times in tool life can be achieved by Ca-treating 303 stainless steel.

It was shown that many factors are the cause for the improvement in tool life through Ca-treatment. The MnS inclusions were more globular in one of the Ca-treated stainless steels which could be more beneficial in chip formation. Ca-modified oxide inclusions were malleable at the tested machining conditions which assisted chip formation, and did not seem to have an adverse effect on tool wear. A lubricating layer was found on the rake surface of the machine tool which consisted of MnS in the case of

the base steel. In the Ca-treated steels, an additional oxide lubricating layer was observed with contents of Ca, Si, and possibly Al measured by EDX. The overall thickness of the lubricating layer of the Ca-treated steels were 8 μm, whereas the base steel had a thickness of 3 μm. This suggests that the oxide layer could be beneficial for the stability of the lubricating layer during machining. These factors are linked to the improved machinability of the Ca-treated 303 stainless steels.

Paper IV: Effect of Grain Refining on Properties of Superaustenitic Stainless Steel

Paper 4 deals with identifying the effect of grain refinement of properties such as: segregation of alloying elements, mechanical properties, machinability, and corrosion resistance. The effect of grain refinement on machinability will be discussed in this thesis. The other material properties can be seen in the full article, or in the Master's thesis of Dustin Arvola. A base steel was compared to a grain refined steel inoculated with Ti, Al, and Mg additions to coprecipitate TiN inclusions on Al_2MgO_4 spinel inclusions. The synergistic effects of grain refinement and addition of abrasive inclusions on the machinability of super austenitic stainless steel was investigated.

The fixed volume machining tests revealed that the refined stainless steel had a decrease of 13% in final flank wear compared to the base steel while machining an equivalent volume of material. The results of the inclusion analysis showed that the refined steel had close to 200 inclusions per unit area, the majority of them being abrasive TiN or spinel inclusions. On the other hand, the base steel had 57 inclusions per unit area. The grain size of the refined steel in the top section of the casting was 2.9 mm compared to 8 mm for the base steel. From the machine chip analysis, the hard TiN and Al_2MgO_4

inclusions fracturing during machining would could contribute to easier chip formation. It seems that the benefit of the finer grain size of the refined steel offset the detrimental effect of increased content of abrasive inclusions.

PAPER

I. EEFECT OF ALIMINUM AND VANADIUM FINE GRAIN PRACTICE ON THE MACHINABILITY OF 4140 STEEL

Mark Emmendorfer*, Simon N. Lekakh, Laura N. Bartlett, Ronald J. O'Malley[#]

Missouri University of Science and Technology

284 McNutt Hall1400 N. Bishop Ave.

Rolla, MO 65409

Geary Ridenour, Eduardo Scheid

Gerdau Special Steel North America

5225 Planters Road

Fort Smith, AR 72902

John Heerema
Gerdau Long Steel North America
1678 Red Rock Road
St. Paul, MN 55119

*Presenting Author email: mcec73@mst.edu

[#]Corresponding Author email: omalleyr@mst.edu

[#]Corresponding Author phone: (573) 341-7683

Keywords: Machinability, 4140, non-metallic inclusions, machining tool life

ABSTRACT

The effect of grain refining practice on the machinability of 4140 steel was investigated using processed bar stock from two industrially produced heats. The first heat employed a vanadium micro-alloy fine grain practice and the second heat employed an aluminum fine grain practice. Progressive flank wear on the machining tool was measured during machining tests to obtain tool life curves for each trial condition. The tool wear was evaluated at three different cutting speeds to produce a Taylor's curve to fully characterize the relative machinability of the two steels. Metallography was performed to document the microstructure and automated SEM/EDX analysis was used

to characterize the non-metallic inclusions in the two steels. The microstructure of the machining chips and the surface condition of the tools after machining were also documented. While both steels possessed a bainitic microstructure, the aluminum treated steel exhibited better machinability than the vanadium treated steel.

1. INTRODUCTION

The definition of machinability is the ease with which a material can be machined while maintaining a satisfactory surface finish. This can be evaluated by several parameters: tool life, tool forces, surface roughness of the workpiece, and chip formation [1]. The tool life criterion is one of the more common practices of defining the machinability of a material [2]. Das et al. [3] studied the machinability of 4140 by measuring tool life as well as surface roughness using different machining parameters to optimize the machining process. Other studies [4-8] investigated the machinability of 4140 and 4142 type steels comparing the effect of Ca-treatment on machinability of the steel. Their findings agree that Ca-treatment improves machinability in multiple ways. A lubricating layer can form during machining of Ca-treated steels on Ti-bearing coated machine tools. The lubricating layer was not found when machining untreated steels, or when machining with uncoated tools [6-7]. Ca-treatment can also form calcium aluminates that tend to be less abrasive than alumina present in Al-killed steels. Calcium aluminate inclusions may also be enveloped by *(Ca,Mn)S* which can further enhance machinability [7]. These complex oxy-sulfide inclusions were present in steels that exhibited better machinability that the other steels present in the studies [6-8]. Different grain refining practices are used in industry to improve properties of 4140 steel, while the effect of these practices on steel machinability was not verified. In this study,

the effects of different non-metallic inclusion populations due to different grain refining practices on 4140 steel machinability was investigated.

2. EXPERIMENTAL MATERIALS AND PROCEDURE

Two industrially produced Ca-treated grades of AISI 4140 steel were used in this study. The steel G1 was produced using a vanadium fine grain practice. G2 was produced using an aluminum fine grain practice. These refining practices made a slight difference in the chemistries because vanadium or aluminum were added. The steel bars were supplied in the as-rolled condition having a diameter of 3.5 inches. Hardness measurements were taken every 0.125 inch through the cross-section of the steel bars. Steels G1 and G2 had consistent hardness values through the cross-section of 28 and 29 HRC respectively. To characterize the microstructure and non-metallic inclusions, samples were then cut in the transverse, labeled T, and longitudinal directions, labeled L. Metallography was done using optical microscopy. The non-metallic inclusion families were characterized using an ASPEX 1020 SEM/EDX with an automated feature analysis to count 2000 inclusions from 4-15 mm^2 area of the sample. An additional inclusion analysis was run targeting only the oxide inclusions, presented in the steel by scanning a large between 25-30 mm^2 of the sample. Data was analyzed using the methods described in work of Harris et al. [9].

The machinability of the steels was quantified by measuring the progressive flank wear at three machining speeds: 460, 655, and 850 SFM (ft/min) to obtain tool life curves with constant 0.005” ipr (inch/rev) feed rate, 0.062” depth of cut, and dry cutting condition. A steel with a better machinability will exhibit lower tool wear and a longer corresponding tool life. The machining tests were completed on a HAAS TL-1 CNC

lathe. The workpiece has a diameter of 3.5 inches, and a machining length of 8.75 inches. A Sandvik Coromant SNMG 432-PM 4325, a *Ti(C,N)+ Al_2O_3* and *TiN* coated cemented carbide tool was used for the machining tests. The oxide surface was removed prior to machining. The progressive flank wear was measured every 3-4 passes using a DinoLite AM 4815ZTL digital microscope. The criterion of tool life was the machining time for a critical tool wear value of 0.15 mm. The machining results were analyzed using Taylor's tool life curve [10]:

$$V_c * T^n = C \tag{1}$$

where: V_c is cutting velocity (m/min), T is tool life (mins), coefficient n = -1/k (k is slope of line on Taylor's tool life curve, and C = constant

Machining chips were collected during the machining tests and were sectioned, polished and examined using SEM/EDX analysis to observe the deformation behavior of inclusions during machining and their influence on chip formation. The flank and rake surfaces of the worn machine tools were also analyzed for evidence of a lubricating layer and to verify the final flank wear of each test. Shear angle was calculated from measured chips thickness using Eq. 2 [11]:

$$\tan\varphi = \frac{t}{T}\cos\alpha \div (1 - \frac{t}{T}\sin\alpha) \tag{2}$$

where: φ is shear angle, t is uncut chip thickness (feed rate), T is measured chip thickness, and α is rake angle of cutting tool. A Dorian tool holder MSRNL 12-4B with a rake angle of -7° determined the rake angle for the machining tests.

3. RESULTS AND DISCUSSION

3.1. MATERIAL CHARATERIZATION

Optical metallography revealed a bainitic structure in of both G1 and G2 steels is the as-rolled condition.

The total concentration of elements of the inclusions present in the steels are listed in Table I. From these results, most of the inclusions are *MnS* in both steels. Steel G2 has an additional inclusion population that is rich in aluminum due to the aluminum fine grain practice. These inclusions are *MnS* with *Al*-rich oxide cores. Both steels have similar area occupied by inclusions. Steel G2 has slightly more inclusions per unit area due to the inclusions being slightly smaller in size.

Table 1: Total Concentration of elements in inclusions, ppm.

Steel	Mg	Al	Si	S	Ca	Mn	Number per mm^2	Area, ppm	Average Diameter, µm
G1	4	2	2	100	5	259	354	755	1.53
G2	1	17		99	9	239	409	759	1.4

From the general analysis of inclusion family, it was shown that the *MnS* inclusions make up most of the inclusions present. However, it is still necessary to consider the oxide inclusions present in the steel so an additional analysis targeting the oxide inclusions by scanning a large area was performed. Since some of the oxide inclusions are associated with the sulfide inclusions, a 10 wt.% S threshold was applied to the data after the analysis to separate free oxide inclusions from oxides associated with sulfide inclusions. Figure 1 shows the total concentration of elements in the oxide

inclusions. Example oxide inclusions in the steel are shown in Figure 2. The oxide inclusions present in steel G1 are rich in *Ca-Si-Al* and tend to be free oxides. The oxides in steel G2 are *Ca-Al* oxides enveloped by *(Mn,Ca)S* inclusions, or present as oxide cores of sulfide inclusions. The total concentration of oxide inclusions in steel G1 is higher than steel G2 due to the oxides in the former steel being associated with the sulfide inclusions.

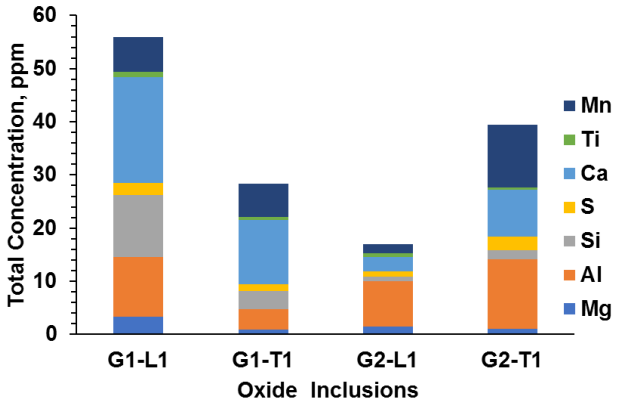

Figure 1: Total area occupied by oxide inclusions in the studied steels.

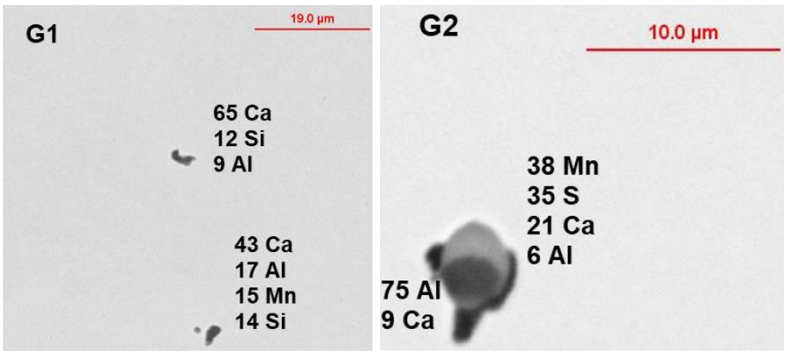

Figure 2: SEM/EDX analysis of oxide inclusions presented in G1 steel (left) and steel G2 (right).

The total concentration of elements in the sulfur bearing inclusions obtained from the additional analysis can be seen in Figure 3. Steel G2 has a noticeable content of aluminum within the sulfide inclusions compared to steel G1. The aluminum is in form of *Al-rich* oxide cores within the *MnS* inclusion or deformed *Ca-Al* oxide inclusions enveloped by *(Mn,Ca)S* inclusions, as stated above. An *Al-rich* oxide core within an *MnS* inclusion can be seen in Figure 4 in steel G2. Some of the inclusions in steel G1 are *(Mn,Ca)S* inclusions that tend to be smaller and much less deformable than pure *MnS*.

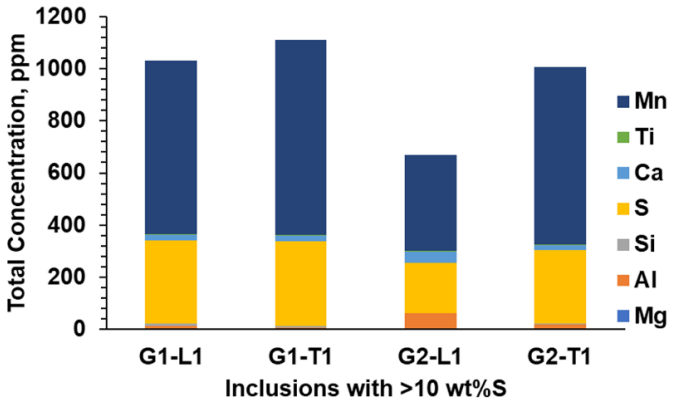

Figure 3: Total concentration of elements in inclusions with greater than 10 wt.% sulfur.

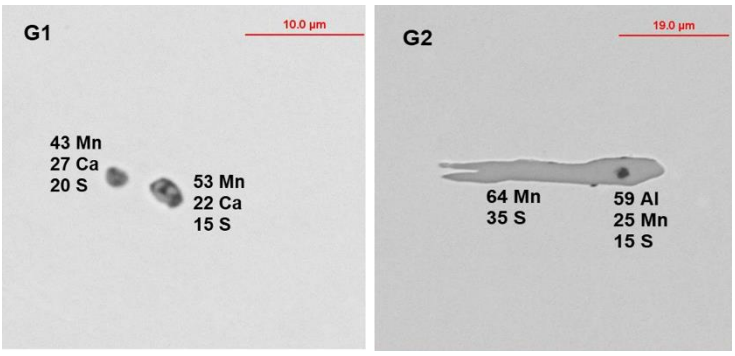

Figure 4: Example sulfide inclusions found in longitude sections of steel G1 (left) and steel G2 (right).

3.2. MACHINING TEST, TOOL AND MACHINE CHIP ANALYSIS

The tests were carried out at 460, 655, and 850 SFM cutting speeds. Flank wear was used as the criterion for quantifying machinability. Some crater wear was observed during machining during all the machining tests; however it was difficult to measure due to the chip breaker geometry of the machine tools. The tool life for each condition was met when the flank wear reached a value of 0.15 mm. For the 655 SFM cutting speed, steel G1 had a 48 minutes tool life of, whereas steel G2 had a significantly longer tool life (76 minutes).

The results of all the machining tests for both steels can be seen in Figure 5. Tool life decreases as machining speed increases for both steels. Steel G2 exhibits better machinability at all studied cutting speeds. The largest difference in tool life is observed at 655 SFM where steel G2 has a 58% increase in tool life compared to steel G1. The tool life of the two steels seem to converge at the higher cutting speed. Experimental coefficients of the Taylor's curves (Eq. 1) shown in Figure 5 were calculated for steels G1 and G2 from the tool life data collected from this study.

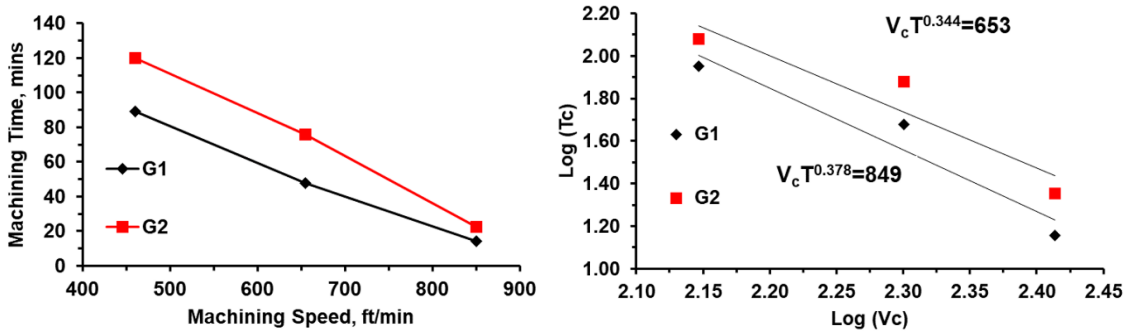

Figure 5: Comparison of tool life at different machining speeds for steel G1 and G2 (left) and Taylor's tool life curves for both steels (right).

Collected at three cutting speeds chips were mounted and polished to analyze the cross-section. Chip thickness and shear angle were calculated according to Eq. 2 can be seen in Figure 6. It can be observed that as cutting speed increases chip thickness decreases and thus shear angle increases due to the increased strain rates encountered at higher cutting speeds. The shear angle for steel G2 is three degrees higher when compared to steel G1at the 460 and 655 SFM cutting speeds. At the cutting speed of 850 SFM, the shear angles of the two steels only differ by 1 degree. This correlates with the large difference in tool life observed at the lower cutting speeds, and the similarity in machinability at the highest cutting speed. Kim and Park [11] also reported a smaller chip thickness and larger shear angle for a stainless steel that had better machinability. A similar trend was indicated by Singh et al. [12] which observed a greater chip thickness for a steel with abrasive oxide inclusions compared to an untreated steel under identical machining conditions.

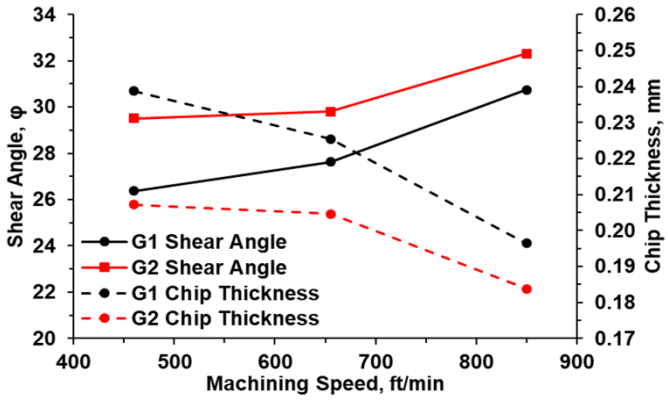

Figure 6: Shear angle and machine chip thickness for steels G1 and G2.

The chemical analysis of the non-metallic inclusions observed in polished cross sections of the collected machining chips is shown in Figure 7. Inclusions observed in the machine chips can be classified into two categories: non-deformable and deformable inclusions. The free oxides present in steel G1 are mostly non-deformable inclusions. An example of such *Ca-Si-Al* oxide inclusion is shown in Figure 7a. During machining, voids formed around the inclusions. The deformable inclusions found in both steels are the *MnS* inclusions. The complex *MnS* inclusions with the *Al-bearing oxide cores of* in steel G2 (Figure 7b) are still deformable during machining. Also, the complex *Ca-Al oxide core* enveloped by *(Mn,Ca)S* inclusions are slightly deformable during machining (Figure 7c). It seems that when the oxide inclusions are enveloped by sulfide inclusions the inclusions appear to behave similarly to the sulfide shells. A possible explanation of the better machinability of steel G2 could be due to the oxides being enveloped sulfide inclusions, and thus their abrasive properties are minimized. Enhanced machinability of steels studied the other authors [8,13] was directly linked to calcium aluminates being surrounded by *(Ca,Mn)S* inclusions. The steels with longer steel life studied in [6-7] contained the similar oxide inclusions enveloped by complex sulfides.

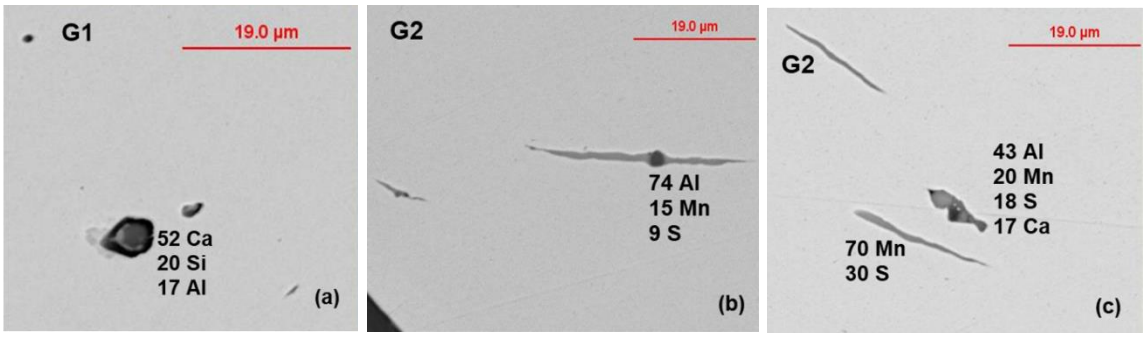

Figure 7: Oxide and sulfide inclusions found in machine chips steel G1 (a) and steel G2 (b, c).

The rake and flank surface of the machine tools were analyzed in an SEM equipped with EDX to investigate lubricating layer formation during machining. Areas near the cutting edge were characterized using EDX. Evidence of *Mn, S, Ca, and Si* is present near the cutting edge of the machine tool in both samples. This deposit is the result of non-metallic inclusions being deposited onto the machine tool from the steel being machined. This deposition can act as a lubricating layer during machining [4-8]. Machine tools from all three machining speeds for both G1 and G2 steels show evidence of this lubricating layer. Some crater wear is also present on the machine tools, suggesting that the lubricating layer might be more beneficial in reducing flank wear than crater wear. This lubricating layer appears to have a positive impact on the machinability of both steels.

4. CONCLUSIONS

Machinability of two industrially produced Ca-treated 4140grade steel with different fine grain refining practices was characterized by measuring tool life. Steel G1 is a vanadium fine grain practice, whereas steel G2 is an aluminum fine grain practice. These different fine grain practices affected the inclusion populations present in the steel. The machinability of steel G2 is significantly better than steel G1 at the 460 and 655 SFM cutting speeds when the tool life was increased 58%. Both steels had similar tool lives at the 850 SFM cutting speed. Both steels have evidence of a lubricating layer on the machining tool at all three cutting speeds. The main difference between the steels is that steel G1 has more free oxides than steel G2. When the calcium aluminate inclusions are enveloped by *(Ca,Mn)S*, the abrasive nature of the oxides during machining tends to be reduced. This may also be true for the *Al-rich* oxide cores within the sulfide inclusions

present in steel G2. Both conditions allow the inclusions to assist in chip formation and reduce the abrasive wear during machining.

ACKNOWLEDGEMENTS

The authors would like to thank the industrial sponsors of the Kent D. Peaslee Steel Manufacturing Research Center for funding this research.

REFERENCES

1. Klocke, F., & Kuchle, A. (2013). *Manufacturing Processes 1 Cutting*. Berlin: Springer.

2. Ånmark, N., Karasev, A., & Jönsson, P. (2015). The Effect of Different Non-Metallic Inclusions on the Machinability of Steels. *Materials,8*(2), 751-783. doi:10.3390/ma8020751

3. Das, S. R., Dhupal, D., & Kumar, A. (2015). Experimental investigation into machinability of hardened AISI 4140 steel using TiN coated ceramic tool. *Measurement,62*, 108-126. doi:10.1016/j.measurement.2014.11.008

4. Hamann, J., Grolleau, V., & Maître, F. L. (1996). Machinability Improvement of Steels at High Cutting Speeds – Study of Tool/Work Material Interaction. *CIRP Annals,45*(1), 87-92. doi:10.1016/s0007-8506(07)63022-4

5. Bittès, G., Leroy, F., & Auclair, G. (1995). The relationship between inclusionary deposits and the wear of cutting tools. *Journal of Materials Processing Technology,54*(1-4), 88-96. doi:10.1016/0924-0136(95)01925-1

6. Kurt Tonshoff, Hans & Cassel, Claus. (1993). Effects of non-metallic inclusions in quenched and tempered steel on the wear behavior of cermet cutting tools. 49. 73-78.

7. Ruppi, S., Ho¨grelius, B., & Huhtiranta, M. (1998). Wear characteristics of TiC, Ti(C,N), TiN and Al2O3 coatings in the turning of conventional and Ca-treated steels. *International Journal of Refractory Metals and Hard Materials,16*(4-6), 353-368. doi:10.1016/s0263-4368(98)00039-0

8. Harju, E., Kivivuori, S., & Korhonen, A. (1999). Formation of a wear resistant non-metallic protective layer on PVD-coated cutting and forming tools. *Surface and Coatings Technology,112*(1-3), 98-102. doi:10.1016/s0257-8972(98)00771-3

9. M. Harris, O. Adaba, S. Lekakh, R. O'Malley, V. Richards: AISTech Proceedings, 2015, pp. 3315–25.

10. ISO 3685:1993. Tool-life testing with single point turning tools.

11. Kim, S., & Park, Y. (2009). Effects of copper and sulfur additions on machinability behavior of high performance austenitic stainless steel. *Metals and Materials International,15*(2), 221-230. doi:10.1007/s12540-009-0221-6

12. Singh, S., Chakrabarti, A., & Chattopadhyay, A. (1997). A study of the effect of inclusion content of the machinability and wear characteristics of 0.24% carbon steels. *Journal of Materials Processing Technology,66*(1-3), 90-96. doi:10.1016/s0924-0136(96)02500-9

13. Rózański, P & Paduch, J. (2003). Modification of non-metallic inclusions in steels with enhanced machinability. Archives of Metallurgy. 48. 285-307.

II. AN INVESTIGATION OF THE MACHINABILITY OF ABRASION RESISTANT AR450 STEEL

Mark Emmendorfer*, Simon N. Lekakh, Laura N. Bartlett, Ronald J. O'Malley[#]

Missouri University of Science and Technology

284 McNutt Hall1400 N. Bishop Ave

Rolla, MO 65409

Rick Bodnar, Sunday Abraham, Yufeng Wang, Matthew Werner
SSAB Americas
1770 Bill Sharp Blvd
Muscatine, IA 52761

*Presenting Author email: mcec73@mst.edu

[#]Corresponding Author email: omalleyr@mst.edu

[#]Corresponding Author phone: (573) 341-7683

ABSTRACT

The machinability of abrasion resistant AR450 steel was examined using industrial steel samples obtained for different process routings including: EAF vs. BOF steelmaking and steady state vs. non-steady state casting conditions. Samples for machinability testing were cut from fully processed AR450 plate samples and a fixed volume machining test was conducted to measure the progressive flank wear of the machining tool during machining evaluations. Machining chip analysis, tool wear measurements, tool surface analysis and microstructural characterization of the steel were performed to investigate factors affecting the machinability of each steel sample. Metallography and cross section hardness testing confirmed the presence of a martensitic microstructure for all samples tested. Automated SEM/EDX analysis was employed to

characterize the non-metallic inclusions present in the steel. Non-metallic inclusions were observed to have a significant influence on the machinability of AR450 steel.

1. INTRODUCTION

The definition of machinability is the ease of a material to be machined. This can be evaluated by several parameters: tool life, tool forces, surface roughness of the workpiece, and chip formation [1]. The tool life criterion is one of the more common practices of defining the machinability of a material [2]. AR450 steel is used in applications that have enhanced requirements for abrasion resistance. One example of the use of this steel is for mining applications. The abrasion resistance is derived from its high hardness of 450HBW Brinell hardness. However, such a high level of hardness has negative effects on machinability. Chinchanikar et al.[3] machined AISI 4340 steel at 35 and 45 HRC (327-421 HBW) hardness levels and reported that the tool life can be doubled by machining the lower hardness workpiece under similar machining conditions. Some studies have looked at steels with abrasive type of precipitates while others look at the effect of steel cleanliness. Faulring et al.[4] reported higher tool wear rates while machining steels with oxide inclusions rich in aluminum compared to steels with glassy inclusions which was due to the retained high hardness of the oxides at higher temperatures. On the other hand, improving steel cleanliness increases mechanical properties while making it difficult to machine. Ånmark et al.[5] investigated the effect of steel cleanliness on steel machinability. They compared three steels of varying cleanliness, and found that the steel with the highest values of oxygen and sulfur had the best machinability due to *MnS* inclusions acting as stress raisers in the primary shear

zone. *This study focused on the influence of cleanliness of industrially produced abrasive resistant AR450 steel on machinability.*

2. EXPERIMENTAL MATERIALS AND PROCEDURE

The specimens for this study were taken from three industrial heats. All studied materials are grades of abrasion resistant AR450 steel. This material is known for its high that makes it exceptional for abrasive environments. All tested steels were heat treated in industrial conditions, including reaustenitizing and water quenching of 2" thickness plates from both surfaces. The studied steels are listed in Table I. The plates were produced by different steelmaking process routes and different casting conditions to investigate the effects of varying levels of steel cleanliness. Specimens S2, S3, and S4 were taken from plates produced using the EAF steelmaking process. Specimens S3 and S4 were taken from the same heat, but specimen S3 was taken from plate produced during the caster startup during non-steady state casting conditions. Reoxidation and entrainment of slag or other undesirable structural features could be expected in this production period. Such material is usually not used for marketable product but was chosen for this study as an extreme case. Specimen S4 was taken from plate made during steady state casting process under normal conditions that is representative of marketable product. Specimens S2 and S4 were taken from similarly produced plates but at different time periods and were chosen to evaluate variations in steel cleanliness during industrial production. Specimen S5 was taken from plate produced using the BOF steelmaking process. This difference in melt practice influences the non-metallic inclusion population present in the plate steel. To summarize, the set of specimens collected for the study machinability reflected different process conditions which could affect steel cleanliness.

Table 1: Industrial Conditions for Collected Specimens

Specimen	Casting Condition	Steelmaking Process
S2	Steady State	EAF
S3	Non-Steady State	EAF
S4	Steady State	EAF
S5	Steady State	BOF

The actual specimens used in the machining studies were 8” diameter disks that were water jet cut from 2” thick hot rolled and heat treated plates. Hardness profile measurements were performed through the thickness of all specimens. These measurements revealed consistent hardness values throughout the machining volume, which extended from each surface to 0.6” below the surface. Samples for metallography and non-metallic inclusion analysis were taken in the transverse (T) and longitudinal (L) directions to characterize the microstructure and inclusions. The non-metallic inclusions were analyzed using an automated ASPEX 1020 SEM/EDX by detecting and characterizing 2000 inclusions in an area of 16-30 mm^2. The collected data was processed using methods described by Harris et al. [6].

The machinability of each of the AR450 steels was investigated using a single point turning method and a fixed volume machining test. Twenty machining passes were performed during each test. The progressive flank wear was measured during face machining using an optical microscope. The cutting parameters were: 0.012” ipr (in/rev) feed rate, 0.03” depth of cut, 270 SFM (ft/min) cutting speed, and coolant were used for the machining tests. Duplicate tests were performed for each specimen to assess the repeatability of the results. The machinability criterion used to assess machinability was final flank wear where lower final flank wear indicates better machinability. The

machining was completed on a HAAS TL-1 CNC lathe. A cemented coated carbide cutting tool SNMG 431-QM 4325 manufactured by Sandvik Coromant was used. The flank wear was measured using a DinoLite AM 4815ZTL digital microscope. Machine chip metallography and post-machining tool analysis were also performed to investigate the influence of inclusions on machining.

3. RESULTS AND DISCUSSION

3.1. MATERIAL CHARACTERIZATION

Optical microscopy revealed that all samples had a martensitic microstructure in the machining volume that was tested.

The total concentration of the elements associated with the inclusion population per unit area (1 mm^2) for specimens S2-S5 is shown in Figure 1. The inclusion morphology statistics are listed in Table II. Specimens S2 and S4 have similar inclusion populations and inclusion statistics. The inclusions in these specimens consisted of *Ca-Al* oxides and *CaS* inclusions. Specimen S3 has twice the amount of aluminum in the inclusions compared to specimen S4 due to the non-steady state casting conditions. An increased amount of magnesium and lower content of calcium is also observed in the inclusions found in the non-steady state condition samples. The inclusions in this specimen were Al_2MgO_4 spinel and *Al-rich* oxide inclusions. The specimen S3 also has a higher number of inclusions per unit area, and lower nearest neighboring distance (NND) which means inclusions were found closer together compared to specimen S4, which could be due to reoxidation. Specimen S5 has an overall lower total ppm content of inclusions compared to the other specimens. The common inclusion in this specimen are spinel, *Ca-Al, Mg-rich* oxide, and *CaS* inclusions. This specimen when compared to

specimen S2 has almost half the number of inclusions per unit area, and an increase of NND of 20 µm. Specimen S5 from BOF route was cleaner when compared to specimens S2-S4 collected from the EAF produced steel. The small amount of *Nb* and *Ti found* in all specimens was generally present as nitride inclusions.

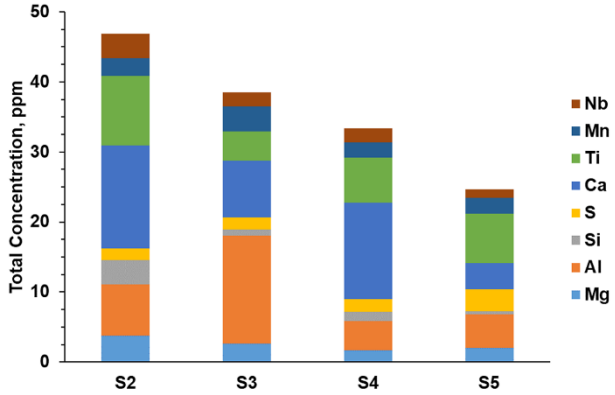

Figure 1: Total concentration of active elements of non-metallic inclusions in specimens S2-S5.

Table 2: Non-metallic Inclusion Statistics

Specimen	Avg. Diameter (µm)	Avg. NND (µm)	Inclusion number, 1/mm²
S2	1.58	66.32	58
S3	1.46	60.97	67
S4	1.41	67.25	54
S5	1.97	86.09	31

3.2. MACHINING TEST RESULTS

The results of the machining tests for specimens S3 and S4 are shown in Figure 2. Specimen S3 was taken from the plate cast under non-steady state conditions which lead to a higher content of abrasive *Al-rich* inclusions compared to specimen S4. Test 1 for

specimen S3 exhibited a slightly higher flank wear rate, and the final flank wear was comparable to specimen S4. However, large visible defects, possibly linked to entrained slag or refractory that was as large as 0.5” in diameter were revealed on the machined surface during the second test of specimen S3. Such defects lead to aggressive tool wear. These defects disappeared after the 9th machining pass, and the resulting tool wear rate reverted back to the wear rate observed in the first test for specimen S3. The increased number of abrasive inclusions and possibly entrained slag had a detrimental effect on machinability. As was mentioned above, the material from non-steady state conditions was taken for this study as extreme case and this condition is not normally found in marketable product.

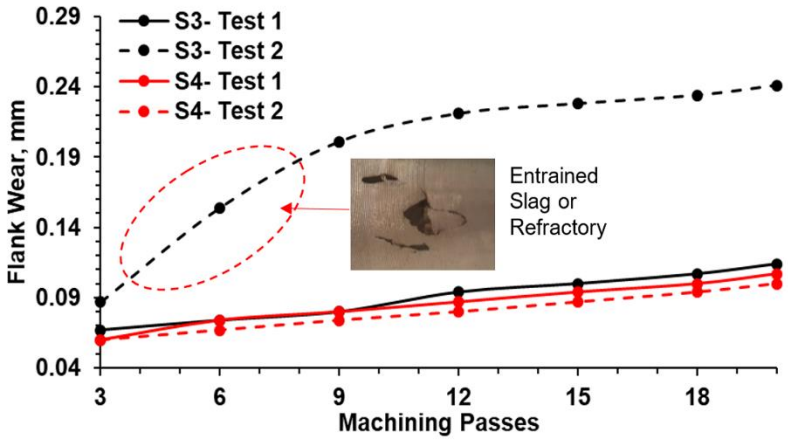

Figure 2: Progressive flank wear results for specimens S3 and S4 steels.

The machinability of the EAF produced steels used for specimens S2 and S4 and the BOF produced specimen S5 are shown in Figure 3. Specimens S2 and S4 had similar final flank wear values as well as the rates of flank wear. Specimen S5 on the other hand

has a more aggressive flank wear rate, which resulted in a much higher flank wear value of 0.16 mm compared to 0.1 mm for the other specimens. This is an increase in flank wear of 60% when comparing specimen S5 to the other studied cases.

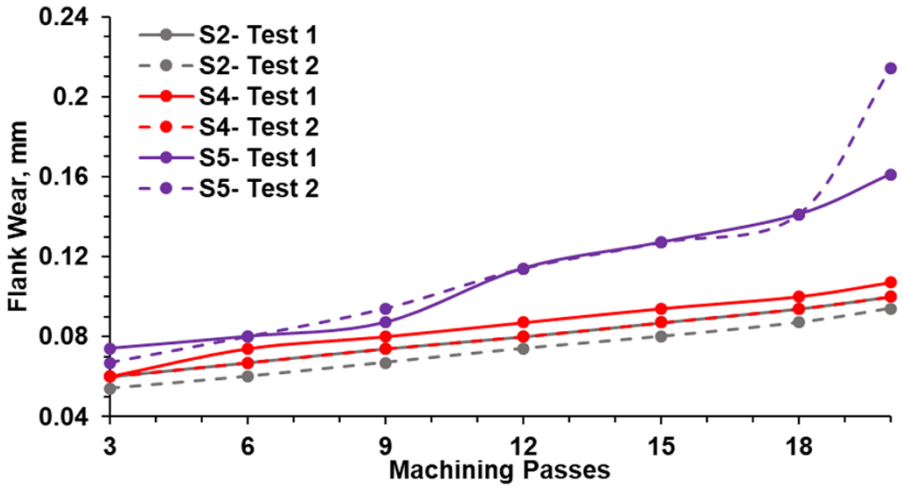

Figure 3: Progressive flank wear results for specimens S2, S4, and S5.

4. DISCUSSION

The role of non-metallic inclusions on machinability of all specimens collected from wear-resistant type AR450 steel produced by different industrial process routes and casting conditions are shown in Figure 4. This plot shows the final flank wear and flank wear rate *vs* the number of non-metallic inclusions per unit area. It reveals that some amount of non-metallic inclusions can be beneficial for machinability of hard wear-resistant steel. Specimens S2 and S4 have similar machinability which is linked to their similar inclusion populations as well as their similar inclusion density. Specimen S2 exhibited the lowest tool wear for machining an equivalent volume of material.

However, larger than optimal inclusion and other hard features content leads to dramatical decrease tool life. The specimen S3 taken during non-steady state condition of casting had twice the amount of aluminum in the inclusions in the form of abrasive Al_2MgO_4 spinel inclusions, and had the most inclusions per unit area. This led to an increase in tool wear rate and final flank wear for specimen S3. Zanatta et al. [7] compared the machinability of steels with different volume fraction of inclusions, and reported that the steels with an increased volume fraction of abrasive inclusions, in their case *Ti(C,N),* had a negative effect on machinability. Their results agree that an increased volume of abrasive inclusions can have a negative influence on machinability.

The other extreme case of interest is the machinability of steels with high levels of cleanliness. Specimen S5 has the largest flank wear rate and resulting final flank wear. When comparing the inclusions per unit area, specimen S5 has half as many inclusions per unit area compared the other steels. This made chip formation difficult, and led to an increase in flank wear rate. Specimen S5 also has the highest inclusion NND of 86 μm compared to specimens S2 and S4 which have NND of about 66 μm, which is another indication of steel cleanliness. Holappa and Helle [8] reported that cleaner steels have poor machinability. While clean steel is beneficial for improved mechanical properties, it can also lead to a decrease in machinability.

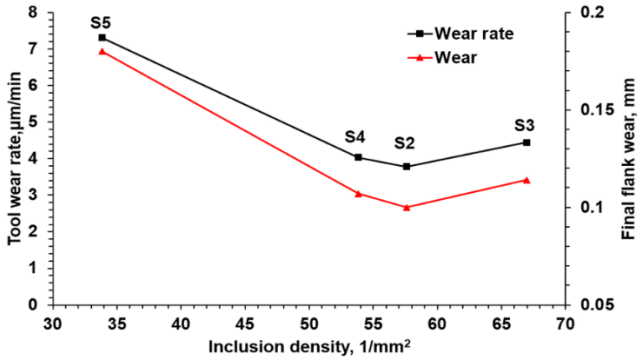

Figure 4: Graph illustrating the effect of inclusions per unit area on tool wear rate.

Machine chips were collected during the machining tests, mounted and polished to look at the cross section of the chips. SEM images of example machine chips of specimens S3, S4, and S5 are represented in Figure 5. The role of inclusion density on machinability is also evident in the machine chips. Specimen S3 has many inclusions visible in the polished cross section of the machine chips. This increased number of abrasive inclusions may have led to the slightly increased final flank wear during machining. Specimen S4 has an intermediate number of inclusions per unit area and this helped facilitate chip formation without comprising an increased flank wear rate. Specimen S5 shows the lowest number of inclusions per unit area which made chip formation difficult which resulted in a poor machinability. The average inclusion diameter in specimen S5 was the largest compared to the other steels which could contribute to the tool wear observed during machining.

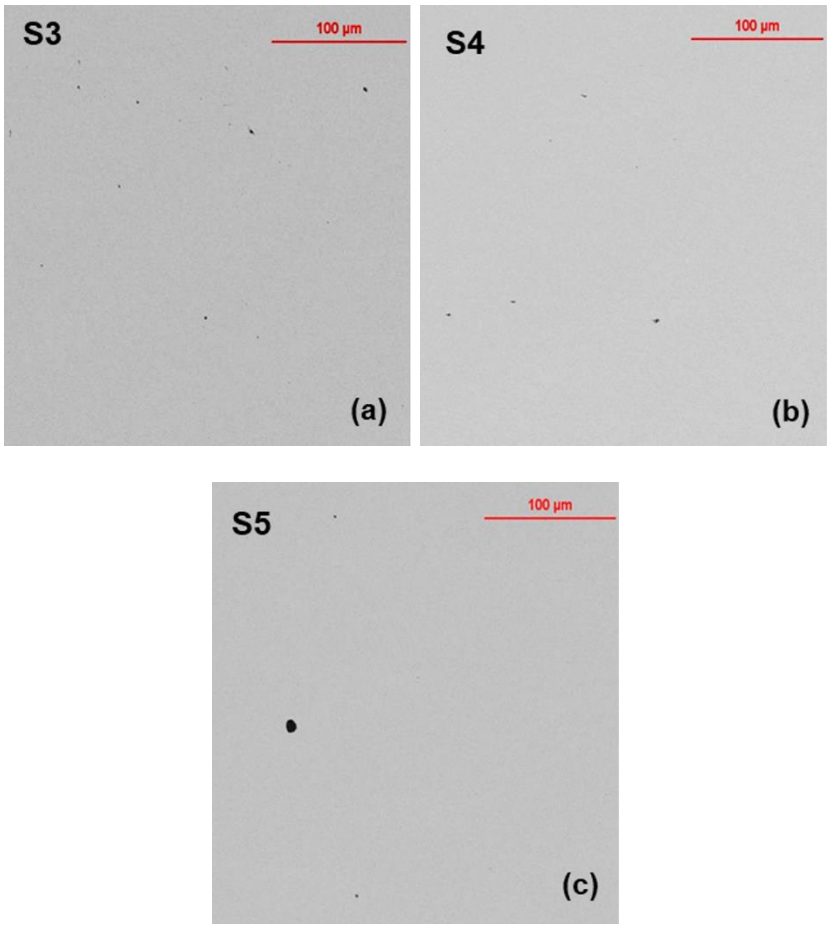

Figure 5: SEM images of machine chips collected during machining test of specimens S3 (a), S4 (b), and S5 (c) cont.

The flank and rake surfaces of the machine tools used during machining were analyzed in an SEM equipped with EDX to characterize the worn surfaces of the tool. Similar wear patterns were found on the all used tools. Calcium-containing deposits were found on the rake surfaces of all cutting tools which has been shown to act as a possible lubricating layer that can form from Ca bearing non-metallic inclusions [9-11]. The use of coolant has been shown to increase tool life up to 200% in some cases [12], but this can also lead to difficulties in tool analysis due to the complex interactions between the

tool and coolant [13]. Cutting fluid was used in this study was to improve tool life, but it also made the post machining tool analysis more difficult to interpret.

5. CONCLUSIONS

The machinability of AR450 has been investigated by measuring the progressive flank during fixed volume machining tests. Specimens taken from steel produced during the non-steady state casting conditions had higher final flank wear due to an increased number of abrasive inclusions present in the steel. Two specimens from two EAF produced steels had similar inclusion populations and exhibited similar machining behavior. Specimen taken from the BOF steelmaking route has fewer inclusions per unit area and a larger inclusion NND when compared to all other studied specimens taken from EAF steel and this difference resulted to a 60% increase in flank wear in the cleaner steel.

ACKNOWLEDGEMENTS

The authors would like to thank the industrial sponsors of the Kent D. Peaslee Steel Manufacturing Research Center for funding this research.

REFERENCES

1. Klocke, F., & Kuchle, A. (2013). *Manufacturing Processes 1 Cutting*. Berlin: Springer.

2. Ånmark, N., Karasev, A., & Jönsson, P. (2015). The Effect of Different Non-Metallic Inclusions on the Machinability of Steels. *Materials,8*(2), 751-783. doi:10.3390/ma8020751

3. Chinchanikar, S., & Choudhury, S. (2013). Investigations on machinability aspects of hardened AISI 4340 steel at different levels of hardness using coated carbide tools. *International Journal of Refractory Metals and Hard Materials,38*, 124-133. doi:10.1016/j.ijrmhm.2013.01.013

4. Faulring, G. M., & Ramalingam, S. (1979). Oxide inclusions and tool wear in machining. *Metallurgical Transactions A,10*(11), 1781-1788. doi:10.1007/bf02811716

5. Ånmark, N., Lövquist, S., Vosough, M., & Björk, T. (2015). The Effect of Cleanliness and Micro Hardness on the Machinability of Carburizing Steel Grades Suitable for Automotive Applications. *Steel Research International,87*(4), 403-412. doi:10.1002/srin.201500243

6. M. Harris, O. Adaba, S. Lekakh, R. O'Malley, V. Richards: AISTech Proceedings, 2015, pp. 3315–25.

7. Zanatta, A. M., Gomes, J. D., Bressan, J. D., & Barbosa, C. A. (2011). Influence of Hard and Soft Inclusions on the Machinability and Polishability of VP100 Mold Steel. *Advanced Materials Research,223,* 464-472. doi:10.4028/www.scientific.net/amr.223.464

8. Holappa, L., & Helle, A. (1995). Inclusion Control in High-Performance Steels. *Journal of Materials Processing Technology,53*(1-2), 177-186. doi:10.1016/0924-0136(95)01974-j

9. Matsui, N., & Watari, K. (2006). Wear Reduction of Carbide Tools Observed in Cutting Ca-added Steels for Machine Structural Use. *ISIJ International,46*(11), 1720-1727. doi:10.2355/isijinternational.46.1720

10. Ruppi, S., Ho¨grelius, B., & Huhtiranta, M. (1998). Wear characteristics of TiC, Ti(C,N), TiN and Al2O3 coatings in the turning of conventional and Ca-treated steels. *International Journal of Refractory Metals and Hard Materials,16*(4-6), 353-368. doi:10.1016/s0263-4368(98)00039-0

11. Kurt Tonshoff, Hans & Cassel, Claus. (1993). Effects of non-metallic inclusions in quenched and tempered steel on the wear behavior of cermet cutting tools. 49. 73-78.

12. El-Hossainy, T. M. (2001). Tool Wear Monitoring Under Dry and Wet Machining. *Materials and Manufacturing Processes,16*(2), 165-176. doi:10.1081/amp-100104298

13. Harju, E., Kivivuori, S., & Korhonen, A. (1999). Formation of a wear resistant non-metallic protective layer on PVD-coated cutting and forming tools. *Surface and Coatings Technology,112*(1-3), 98-102. doi:10.1016/s0257-8972(98)00771-3

III. MODIFICATION OF INCLUSIONS TO ENHANCE MACHINABILITY OF RESULFURIZED 303 STAINLESS STEEL

Mark Emmendorfer*, Simon Lekakh*, Laura Bartlett*, and Ronald O'Malley*

*Missouri University of Science and Technology, Rolla, MO, USA, 65409

Corresponding author E-mail: mcec73@mst.edu

Keywords: 303 stainless steel, machining, machinability, *Ca*-treatment, inclusions

ABSTRACT

To achieve superior machinability of austenitic stainless steel, the effect of modification of non-metallic inclusions in resulfurized 303 stainless steel was investigated. Inclusion modification was performed by varying *Ca*-additions in two industrially produced trial heats. Comparative machining tests were performed on hot rolled bar stock and tool life testing was evaluated by measuring the progressive flank wear of the cutting tool during machining. The machinability of the *Ca*-treated steels was compared to the machinability of an industrially produced baseline 303 steel heat without *Ca*-modification. An automated SEM/EDX analysis was used to analyze and classify the non-metallic inclusions in the steel. Machining chips and deposits on the worn tools were also investigated. The results show that machinability of resulfurized stainless steel can be significantly improved by non-metallic inclusion modification with calcium. The mechanisms that lead to the improvements in machinability are discussed.

1. INTRODUCTION

The definition of machinability is the ease with which material can be removed from a part while maintaining an acceptable surface finish. Machinability can be evaluated by several parameters: tool life, tool forces, surface roughness of the workpiece, and chip formation.[1] The tool life criterion is one of the more common methods of defining the

machinability of a material.[2] Austenitic stainless steel is known for its superior corrosion resistance and mechanical properties. It is also known to be one of the most difficult materials to machine due to its high work hardening, high toughness, and gumminess during machining.[3] It is well established that sulfur can be added to steel to improve machinability. Sulfur combines with *Mn* to form *MnS* inclusions that act as stress risers in the primary shear zone of the cut, promoting chip formation and increasing tool life.[4] This is the reason that 303 resulfurized stainless steel is used in applications that require significant amounts of machining.

Li and Wu[5] compared the machinability of a conventional austenitic stainless steel with a stainless steel modified by free-cutting additives such as of *S*, *Bi*, and *Cu* and reported that the free-machining steel had lower flank wear on the machining tool. This improved machinability was linked to the lubricating layer observed on the rake surface of the cutting tool. Tool surface lubrication provided a longer tool life and lower cutting forces when machining the free-cutting steel. Akasawa et al.[6] studied free cutting additions of *S*, *Cu*, *Ca*, and *Bi* to 303, 304, and 316 stainless steels. They studied the surface roughness of the machined surface, tool wear, and cutting forces as measures of machinability. They found that sulfur and copper additions resulted in lower cutting forces. They also reported that calcium treated steels with Anorthite oxide inclusions had better surface finished and lower cutting forces compared to conventional austenitic stainless steel. An additional study by Bletton et al.[7] investigated the effect of *Ca*-treatment on oxide inclusions targeting Anorthite inclusions in 316L stainless steel. They found that Anorthite inclusions were more deformable during machining, and formed a lubricating layer to promote better machinability. Fang and Zhang[8] also reported improved tool life, chip breakability, and

lower cutting forces while machining a *Ca-S* free-machining stainless steel compared to a conventional stainless steel. However, many aspects of the mechanisms behind improvement of machinability of *Ca*-treated resulfurized austenitic stainless steel are still not clear. *The present study investigates the effects of Ca-treating on the machinability of 303 resulfurized stainless steel through modification of the non-metallic inclusion population.*

2. EXPERIMENTAL MATERIALS

2.1. MATERIAL CHARATERIZATION

AISI 303 stainless steel is used in applications requiring large amounts of machining due to its high machinability compared to conventional stainless steels. Three industrially produced grades of AISI 303 resulfurized stainless steel were used in this study. The chemistries are shown in Table 1. The base steel in this study is denoted by N1. Two grades of Ca-treated 303 stainless steel with different resulting non-metallic inclusion populations are denoted as N2 and N3. The material tested in this study was hot-rolled bar stock that was peeled to a 108 mm diameter bar. The bars were then sectioned to lengths of about 240 mm long for the machinability tests. Cross-sections of this material were used to obtain samples for non-metallic inclusion analysis in the transverse (T) and longitudinal directions (L).

Table 1: Chemistry of studied steels, wt. %.

Specimen	C	Mn	Si	Cr	Ni	Mo	Cu	N	P	S	Ca	Fe
N1	0.05	1.86	0.54	17.10	8.55	0.26	0.31	0.040	0.028	0.32	-	Bal.
N2	0.06	1.88	0.55	17.13	8.55	0.33	0.31	0.026	0.029	0.33	0.002	Bal.
N3	0.04	1.80	0.61	17.08	8.46	0.27	0.32	0.035	0.029	0.32	0.003	Bal.

Samples for the non-metallic inclusion analysis was analyzed on an ASPEX 1020 SEM/EDX system with automated feature analysis to characterize 2000 inclusions from an area of 0.5-3 mm^2 from each specimen. This scanned area is low due to the large number of MnS inclusions present from the steelmaking resulfurization treatment. An additional analysis was run to target only the oxide inclusions in the samples by scanning a larger area of 20-30 mm^2. An adjusted contrast was used to exclude the lower contrast MnS inclusions in the back scattered electron detector image. Data was analyzed using the methods described by Harris et al.[9] To observe the 3D non-metallic inclusion morphology, electrolytic dissolution was performed on steel samples to extract the inclusions and collect them on polycarbonate filter paper, similar to methods outlined by Adaba et al.[10] The electrolytic solution consisted of 2 vol.% triethanolamine, 1 vol.% tetramethyl ammonium chloride in a methanol solution. The extracted inclusions were then analyzed using SEM/EDX analysis.

2.2. MACHINABILITY TESTING, TOOL AND MACHINE CHIP ANALYSIS

The tool-life tests were completed on a HAAS TL-1 CNC lathe. A Sandvik Coromant SNMG 432-MM 1125 coated cemented carbide insert was used. The machinability of the steels was quantified by measuring the progressive flank wear during

the tool-life machining test. The machining specimen is shown in Figure 1. The outer surface of the workpiece was removed prior to testing. The parameters for the tool-life tests were kept constant and are as follows: 200 m min^{-1} machining speed, 1.57 mm depth of cut, 0.2 mm rev^{-1}, and dry cutting condition. The progressive flank wear was measured every few passes with a DinoLite AM 4815ZTL digital microscope. A critical flank wear value of 0.07 mm was used as the tool-life criterion. A steel with better machinability has a longer tool life.

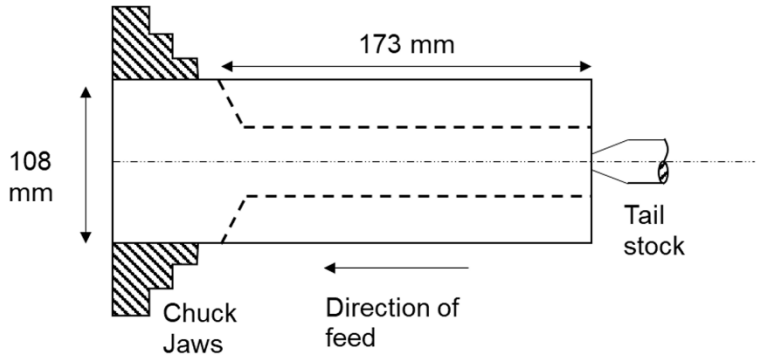

Figure 1**:** Specimen for machining tests.

An additional short machining test was performed for each steel to investigate the initial formation of the lubricating layer that was observed on the cutting tool. This additional test used the same procedure employed previously, but the objective was to observe the initial formation of the lubricating layer during the first 10 minutes of machining. During these tests, the cutting tool was analyzed with a high-resolution SEM/EDX analysis after each machining pass to measure the flank wear and characterize the lubricating layer on the rake surface of the cutting tool. After the SEM analysis, the

tool was placed back into the machine to complete another machining pass. This procedure was repeated until the fourth pass, then four additional machining passes were made and a final examination was conducted on the 8th pass.

Worn surfaces of machine tools used in the machine tests were analyzed to characterize the lubricating layer on the rake surface of the machine tool. The formation of this lubricating layer was investigated using SEM/EDX to characterize the deposit layers on the rake surface of the machine tool after each machining pass. Focus Ion Beam (FIB) milling and high-resolution 3D optical profilometry were also used to measure the developing lubricating layer.

Machine chips were collected during the tool-life tests to study the behavior of the non-metallic inclusions during machining. The machine chips were mounted and polished to view their cross section. The thickness of the chips was measured and the shear angle was calculated according to *Eq.* 1[11]*:*

$$\tan\varphi = \frac{t}{T}\cos\alpha \div (1 - \frac{t}{T}\sin\alpha) \quad (1)$$

where: φ is calculated shear angle, t is uncut chip thickness (feed rate), T is chip thickness, and α is rake angle of cutting tool. A Dorian tool holder MSRNL 12-4B with a rake angle of -7° determined the rake angle for the machining tests.

3. RESULTS AND DICUSSION

3.1. NON-METALLIC INCLUSION ANALYSIS

The non-metallic inclusions in the longitudinal direction can be seen in Figure 2. The majority of the inclusions are *MnS* inclusions that were elongated during hot-rolling. Oxide inclusions are also visible in the Ca-treated steels N2 and N3. It can also be seen that the non-metallic inclusions in N3 are smaller than in the other two steels.

The total concentration of elements within the non-metallic inclusions observed in a 1 mm^2 area is shown in Figure 3. The results show that the majority of the non-metallic inclusions in the steels are *MnS*. During the EDX analysis of *MnS* inclusions observed in the polished sections, it was noted that these inclusions also had some amount of *Fe* and *Cr* (<10 wt%) in solid solution in the inclusions.

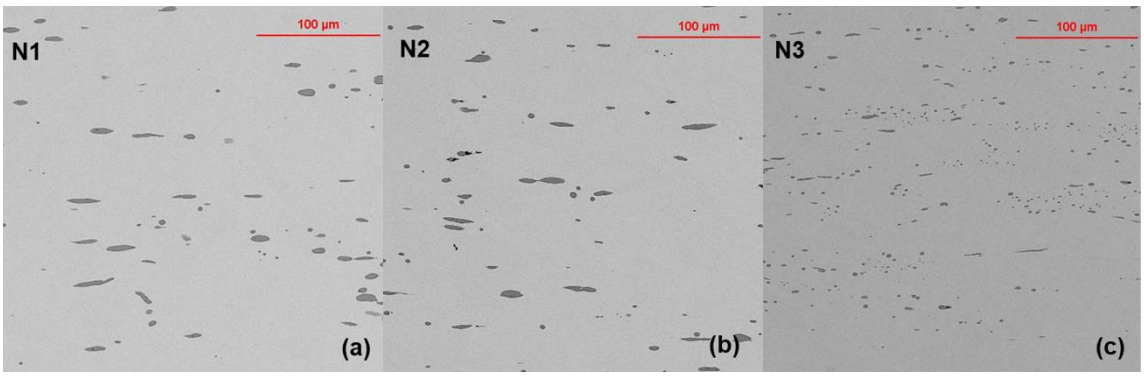

Figure 2: Non-metallic inclusions in longitude directions of bars from three studied steels: N1 (a), N2 (b), and N3 (c).

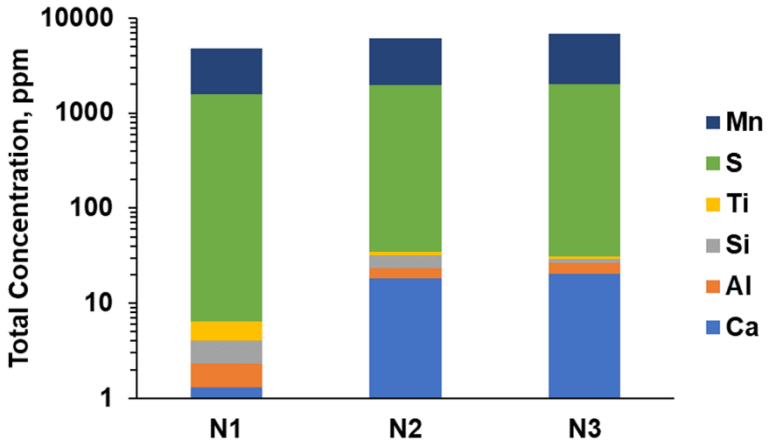

Figure 3: Total concentration (ppm) of elements within non-metallic inclusions.

To isolate the effect of the *Cr-Ni* matrix from the inclusion analysis, several methods illustrated in Figure 4 were employed and their results compared. Conventional EDX analysis of the polished inclusion section (a), FIB trenching to isolate the inclusion (b), and EDX analysis of the extracted inclusions (c). The EDX results for each method are listed in Table 2. During the FIB analysis, the EDX was taken while trenching one side and also from two sides to attempt to isolate the sulfide inclusion from the matrix during analysis. The conventional and FIB analyses revealed similar results, with approximately 10 wt.% Cr and between 10-14 wt.% Fe in the sulfide inclusion. The corresponding concentration of *Fe* and Cr in the extracted sulfide inclusion shown in Figure 5c can be seen in Table 2. This analysis suggests that the sulfide inclusion contains about 7 wt.% *Cr* and <0.5 wt.% *Fe*, which is less than the levels observed using FIB analysis. The differences could be due the electron beam signal interacting with the matrix material in the FIB cavity, or from selective loss of Fe from the inclusion during extraction. In either case, the analysis shows that there is some solid solution of *Cr* in the *MnS* inclusions.

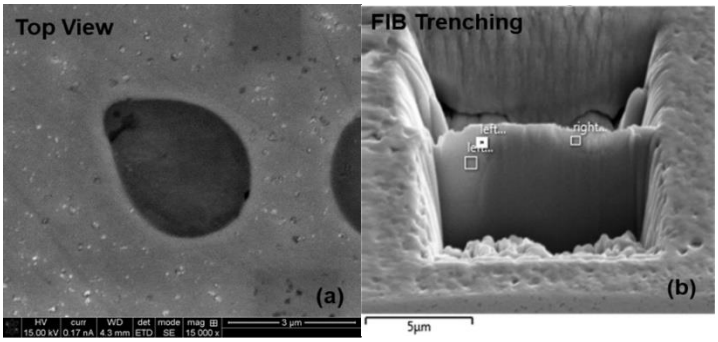

Figure 4: Comparison of methods used for analyzing non-metallic inclusions conventional top view analysis (a), FIB trenching from both sides (b), and extraction of non-metallic inclusions (c).

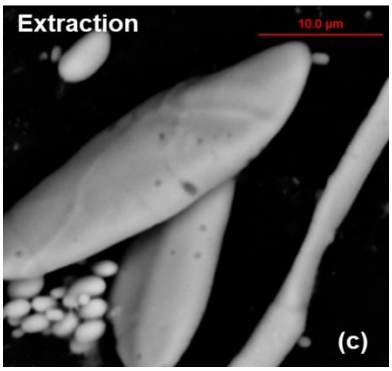

Figure 4: Comparison of methods used for analyzing non-metallic inclusions conventional top view analysis (a), FIB trenching from both sides (b), and extraction of non-metallic inclusions (c) cont.

Table 2: Comparison of Different Analysis of Elements in Sulfide Inclusions, wt. %.

SEM/EDX Method	Cr	Fe	Mn	S	Cr/Fe Ratio
Top View	7.6	10.7	55.2	33	0.71
FIB One side	10.7	14.8	52.1	21.4	0.72
FIB Two side	9.9	12.1	52.9	23.1	0.82
Extraction	7.3	0.4	50.5	35	9.9

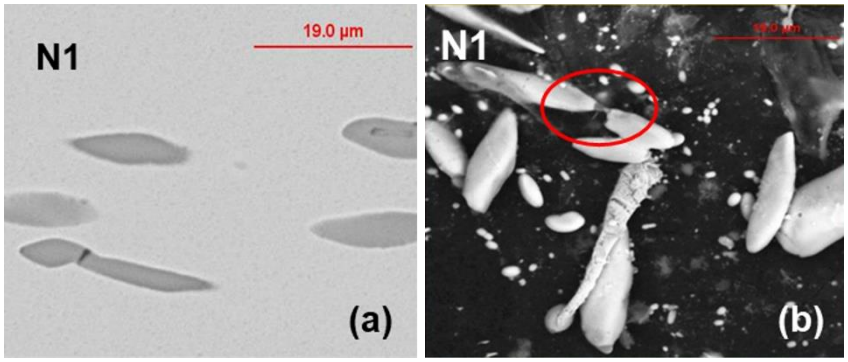

Figure 5: Comparison of non-inclusion morphology in polished 2D section (a and c) with 3D extracted (b and d) in steel N1 (a and b) and steel N3 (c and d). *MnS* inclusions are light grey and oxides inclusions are darker.

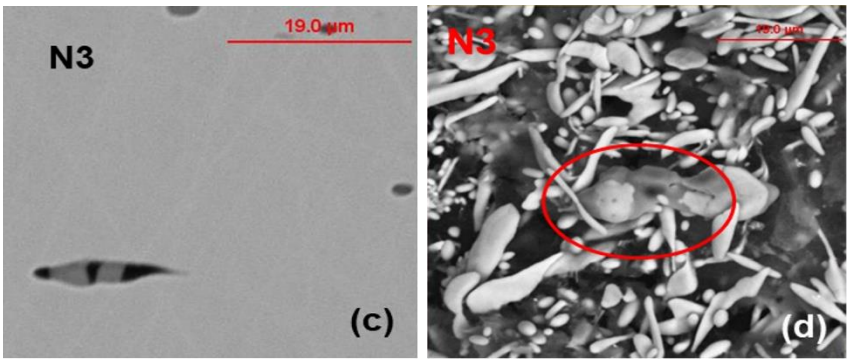

Figure 5: Comparison of non-inclusion morphology in polished 2D section (a and c) with 3D extracted (b and d) in steel N1 (a and b) and steel N3 (c and d). *MnS* inclusions are light grey and oxides inclusions are darker cont.

The *Ca*-treated steels N2 and N3 show a slightly higher total ppm of inclusions compared to the base sample N1 as seen in Figure 3 and steels N2 and N3 have significant amount of *Ca* in the inclusions. While the Mn in the inclusions was mainly associated with sulfides, some manganese was found along with aluminum, silicon, and calcium in the oxide inclusions. An additional analysis using an adjusted contrast threshold was performed to characterize the oxide inclusions, which were much less numerous than the MnS inclusions. The oxide inclusions analysed by this method excluded both sulfides and oxy-sulfides. A composition threshold of 10 wt.% *S* was also applied to the data after the analysis to obtain only oxide inclusions. *Ca*-treatment modified the oxide inclusions to be deformable during hot-working and machining. The total concentration of elements within the oxide inclusions in ppm are presented in Figure 6. *Ca*-treatment increases the oxide inclusion population when comparing N1 to N2 and N3. When comparing the *Ca*-treated steels, N2 had a higher content of *Mn*, while steel N3 had a higher content of *Ca* in the oxide inclusions. Figure 5 shows some SEM images of inclusions in the as-polished 2D plane along with extracted inclusions to show the 3D

morphology of the inclusions. The oxide inclusions in steel N1 were much less numerous and connected multiple sulfide inclusions as observed in Figure 5b. The *Ca*-treated steels had an increased amount of oxide inclusions that were present as free oxides and oxides that resided on the tails of the oxy-sulfide inclusions as seen in Figure 5b and Figure 5c. The modified oxide inclusions appear to be deformable, which could be beneficial for machinability.

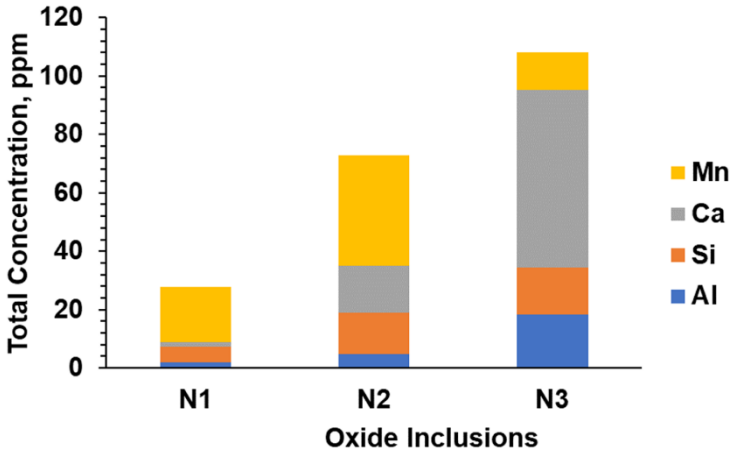

Figure 6: Total concentration (ppm) of elements in oxide inclusions.

Size distributions presented in Figure 7 were measured on polished samples using SEM automated feature analysis. The distributions represented in Figure 7 were measured in the longitudinal (rolling) direction. The size distribution for specimen N1 is much wider compared to the *Ca*-treated steels. The calcium treatment tended to globularize the *MnS* inclusions which can be seen in the SEM images. This led to a decrease in the average inclusion diameter for specimen N3 in the longitudinal direction.

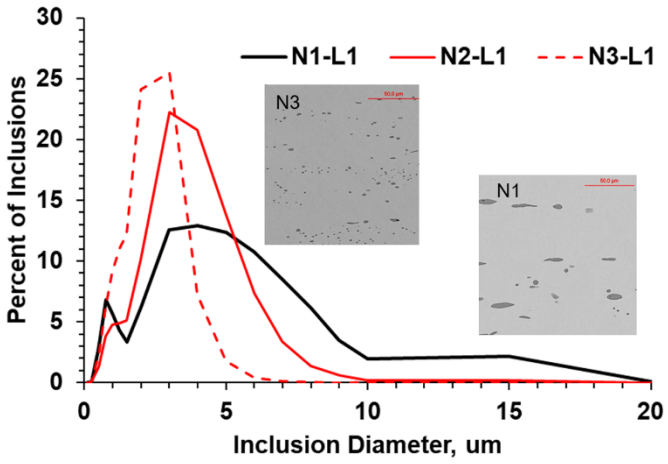

Figure 7: Inclusion Diameter in longitudinal samples for specimens N1, N2, and N3.

3.2. MACHINING RESULTS

The initial stages of machining were investigated to observe the formation of the lubricating layers which was found on the rake surface of the machine tools. The results are shown in Figure 8. The measured flank wear and wear rate for the *Ca*-treated steels are significantly lower. The machinability of the steels are as follows: specimen N3 showing the lowest flank wear, followed by N2, and lastly N1 having the highest flank wear.

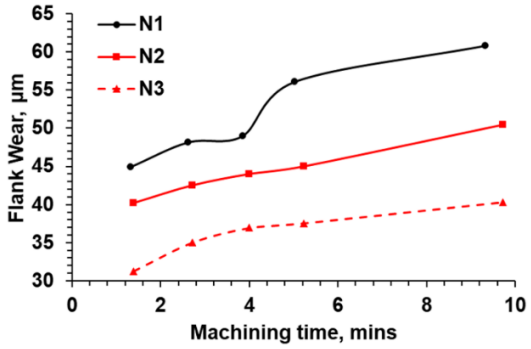

Figure 8: Flank wear results for initial wear machining tests.

The progressive flank wear results for the tool-life tests can be seen in Figure 9. Both *Ca*-treated steels show a significantly longer tool life. When comparing specimen N2 to N1 tool life was increased 3.5 times. When comparing specimen N3 to N1 an increase of almost 5 times in tool life was observed.

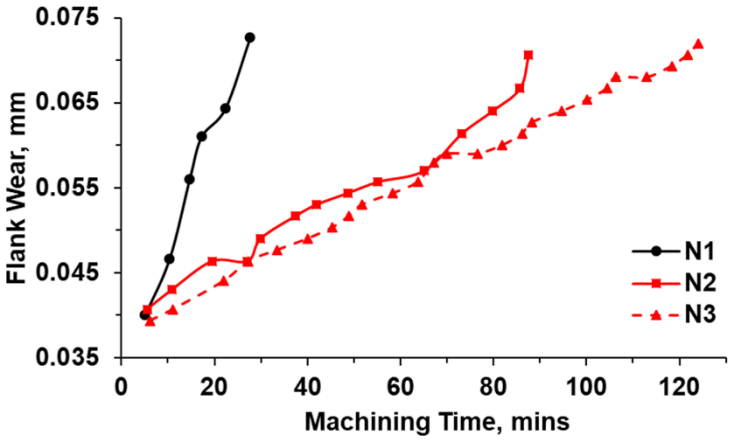

Figure 9: Machining results for tool-life tests. Critical tool wear of 0.07 mm used as tool life criterion.

The lubricating layers on the rake surface of the machine tools were characterized using an SEM equipped with EDX. The presence of a lubricating layer can reduce tool wear during machining. The layer can also resist crater wear by acting as a diffusion barrier at high cutting speeds. Desaigues et al.[12] observed a lubricating layer consisting mainly of *MnS* inclusions while machining a low carbon re-sulfurized steel. Previous studies[8,13,14] found a lubricating layer consisting of *Ca*, *Al*, *Si*, *Mn*, and *S* originating from both oxide and sulfide inclusions while machining *Ca*-treated steels. The SEM images in Figure 10 illustrate the different lubricating layers observed on the machining tools used in the current work after the 3rd machining pass. For steel N1, a *MnS* layer was

found on the rake surface of the cutting tool. In the case of the *Ca*-treated steels N2 and N3, an additional lubricating layer was observed containing oxides of *Ca*, *Si*, and *Al* labeled "oxide layer" in the SEM images shown in Figure 10. The complex oxide layer is comprised of elements found in oxide inclusions in the steel, but the cutting tool also has an *Al*-doped coating which could interfere with the *Al* detected in the EDX analysis.

After about 7 minutes of additional machining time, the tool surfaces were analyzed again. The SEM images for this case are shown in Figures 10d (N1), 10e (N2), and 10f (N3). It is apparent that the lubricating layers continue to build up as more inclusions are deposited onto the tool. The oxide layers on the machining tools for the *Ca*-treated steels appear to be covered by a *MnS* layer as more inclusions are deposited onto the tool as machining continues. This likely occurs because *MnS* inclusions greatly outnumber the oxide inclusions in the steel.

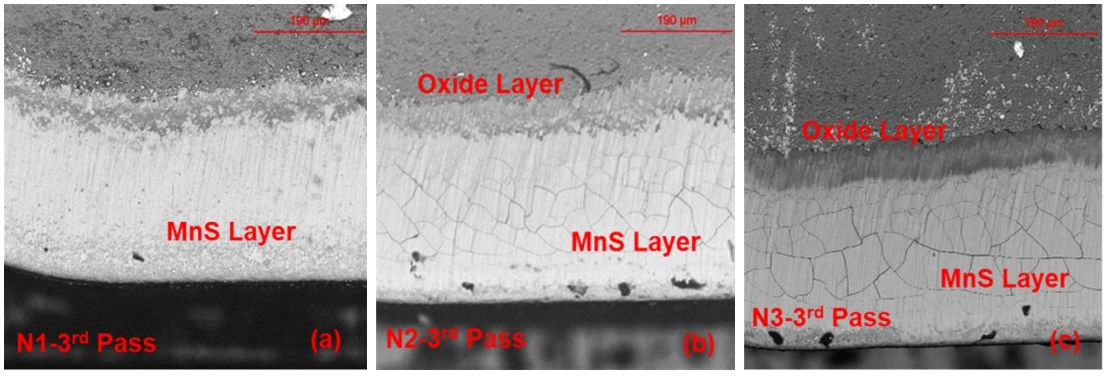

Figure 10: SEM images of the rake surface of machine tools used for initial wear test: after the 3rd machining pass N1 (a), N2 (b), and N3 (c); after 8th machining pass N1 (d), N2 (e), and N3 (f).

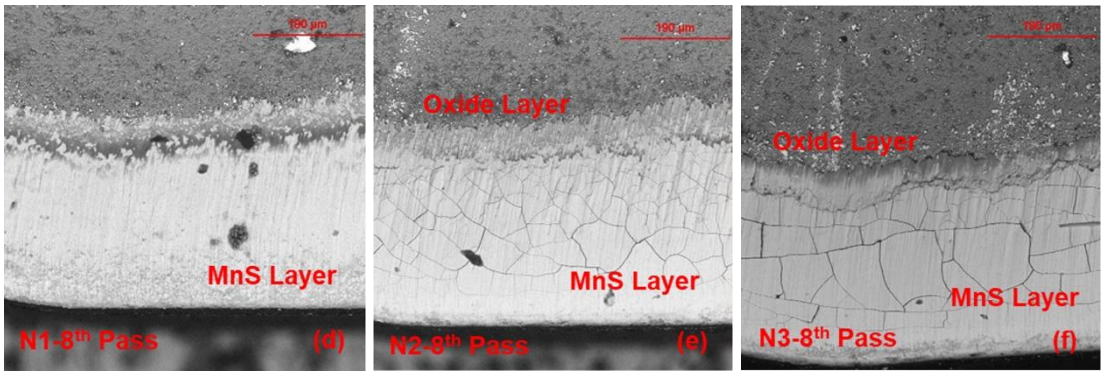

Figure 10: SEM images of the rake surface of machine tools used for initial wear test: after the 3rd machining pass N1 (a), N2 (b), and N3 (c); after 8th machining pass N1 (d), N2 (e), and N3 (f) cont.

The thickness of the lubricating layer was measured with an optical profilometer, and then verified by using a FIB sectioning technique to trench through the lubricating layer and measure the layer thickness. Figure 11 shows the results of the FIB method (a) and the optical profilometer method (b). The thickness of the lubricating layer was measured to be 6.5 μm using the FIB, and was found to be 8 μm in thickness using the optical profilometer. The optical profilometer appears to provide the resolution needed to measure the thickness of the lubricating layer directly. The thickness results for the lubricating layers shown in Figure 10 are in listed in Table 3. The Ca-treated steels appear to have a thicker and more stable lubricating layer of about 8 μm in thickness, whereas sample N1 only has a 3 μm thick lubricating layer after machining an equivalent amount of material.

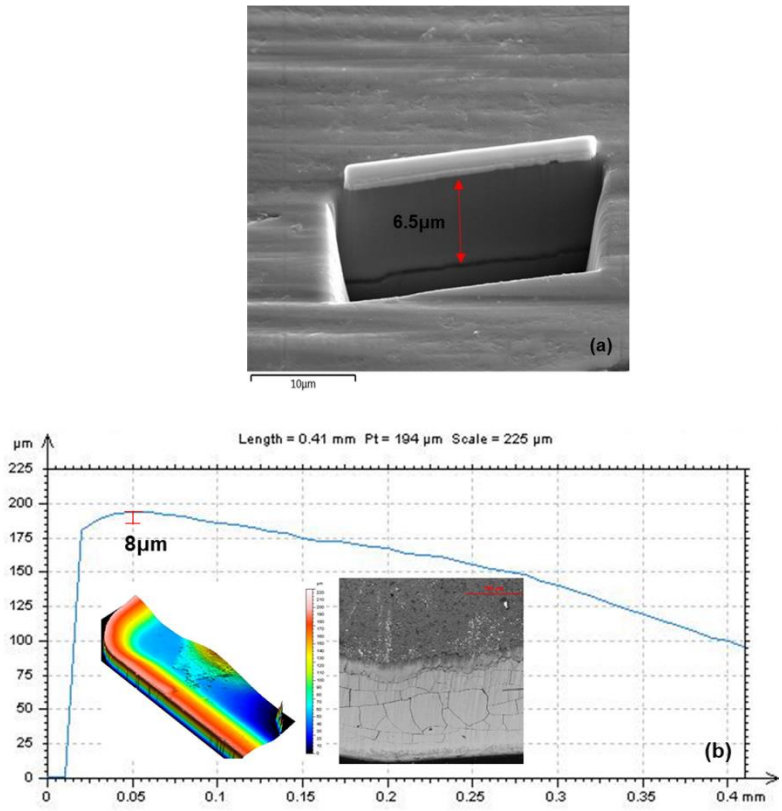

Figure 11: Verification of lubricating layer thickness by FIB trenching method (a) and using optical profilometer (b).

Table 3: Thickness of the Lubricating Layer for the Short Machining Test Tools

Specimen	**Lubricating Layer Thickness**
N1	3 µm
N2	8 µm
N3	8 µm

4. DISCUSSION

Experimental results showed that *Ca*-treatment of resulfurized 303 stainless steel can greatly improve machinability. The behavior of inclusions during machining was

observed in the machining chips (Figure 12a (N1), 12b (N2), and 12c (N3). *MnS* inclusions in all three steels readily deformed during machining, assisting chip formation. This is one of the benefits that sulfide inclusions provide during machining. The other benefit is the ability of MnS inclusions to be extruded onto the rake surface of the machining tool to form a lubricating layer. In the case of the *Ca*-treated steels N2 and N3, the Ca-bearing oxide inclusions also deformed during machining. *Ca*-treatment modifies the oxide inclusions to be more malleable at the temperatures encountered during machining. These oxide inclusions can be heavily deformed, as shown in Figure 12c, which is beneficial for chip formation.

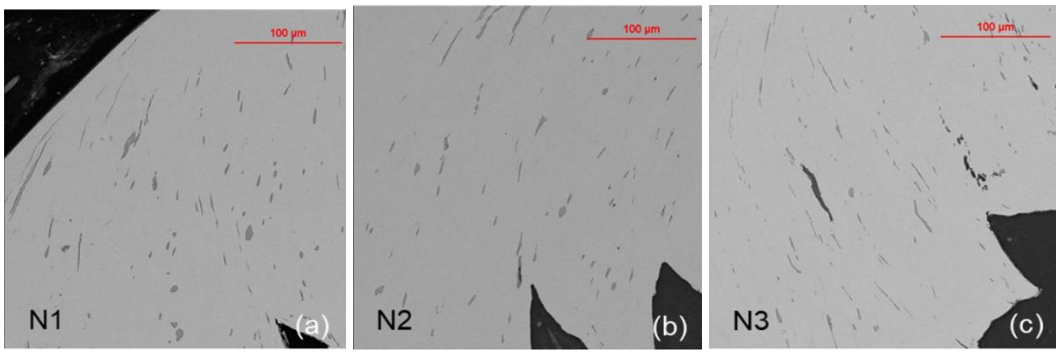

Figure 12: SEM images of polished cross sections of machine chips from N1 (a), N2 (b), and N3 (c).

The thickness of the machining chips was measured and the shear angle for each specimen was calculated using Eq. 1. The results are shown in Figure 13. Segmented chips are encountered at higher cutting speeds, and these types of chips were found for all three steels. The calculated shear angle for N1 and N2 are quite similar in the machining chips analyzed. On the other hand, specimen N3 has an increase in shear angle of two

degrees for the same machining conditions. This increase in shear angle could be due to the increased total ppm of oxide inclusions and modification of the shape of *MnS* inclusions in specimen N3. Kim and Park[11] investigated the machinability of austenitic stainless steels with *Cu* and *S* additions, while also measuring machine chip thickness and reported that the steels with better machinability showed a decrease in chip thickness and thus an increase in shear angle.

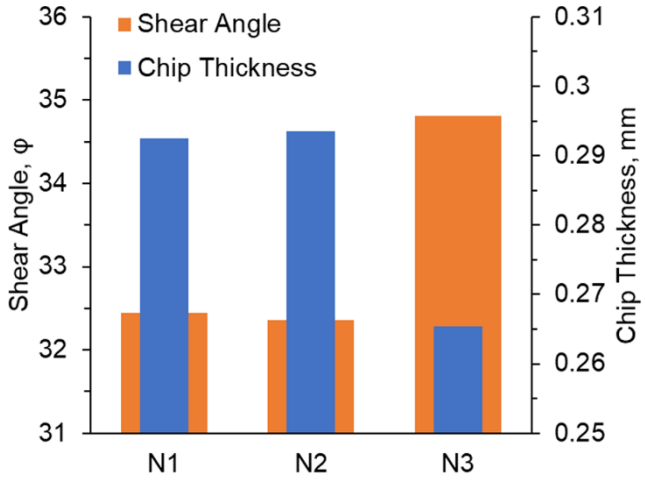

Figure 13: Calculated shear angle and measured chip thickness from machine chips.

There are other factors that could contribute to the observed improvements in machinability that could be attributed to *Ca*-treatment. One factor is the increase in the total ppm of inclusions present in the steel that may be beneficial for chip breaking. *Ca*-treatment also modified the shape and decreased the size of the *MnS* inclusions in the rolling direction. Jiang et al[15] studied the machinability of different free machining austenitic stainless steels and found that a decrease in the shape factor (more globular)

inclusions were better for chip formation because of voids formed during chip formation that reduced flank wear.

It was shown that the oxide inclusions modified by *Ca*-treatment was beneficial for machinability. The average composition of the oxide inclusions for all three steels were measured using extracted oxide inclusions and plotted on the ternary phase diagrams shown in Figure 14. Due to different content of *Mn* in the oxide inclusions in specimens N1 and N2, the results were plotted on the CaO-SiO_2-MnO ternary fixed at 15 wt.% Al_2O_3. Specimen N3 heavily treated by *Ca* was plotted on the CaO-SiO_2-Al_2O_3 phase diagram. The average compositions of the complex oxide inclusions were recalculated to fit the corresponding ternary phase diagrams. This was done as an attempt to approximate the liquidus temperature the oxide inclusions present in the steels. It has been shown that lower melting oxide inclusions are more malleable at machining temperatures which can positively influence the machinability. Oxide inclusions in the Gehlenite and Anorthite regions of the phase diagram are the targeted regions to for best machinability reported by previous studies.[7,13] Specimen N2 has oxide inclusions that fall within the Galaxite phase field which has a similar liquidus temperature compared to Gehlenite. Oxide inclusions in specimen N3 fall within Ca_2SiO_4 phase field, but is close to the Gehlenite phase field. The oxide inclusions in specimen N1 consisted of mainly *Mn*-*Si* with some *Al* and *Ca*, but being plotted on the ternary phase diagram can only be approximated and further study needs to be done. The *Ca*-treated oxide inclusions in specimens N2 and N3 agree with the previous studies[7,13] that an increase in tool life was observed by *Ca*-treatment.

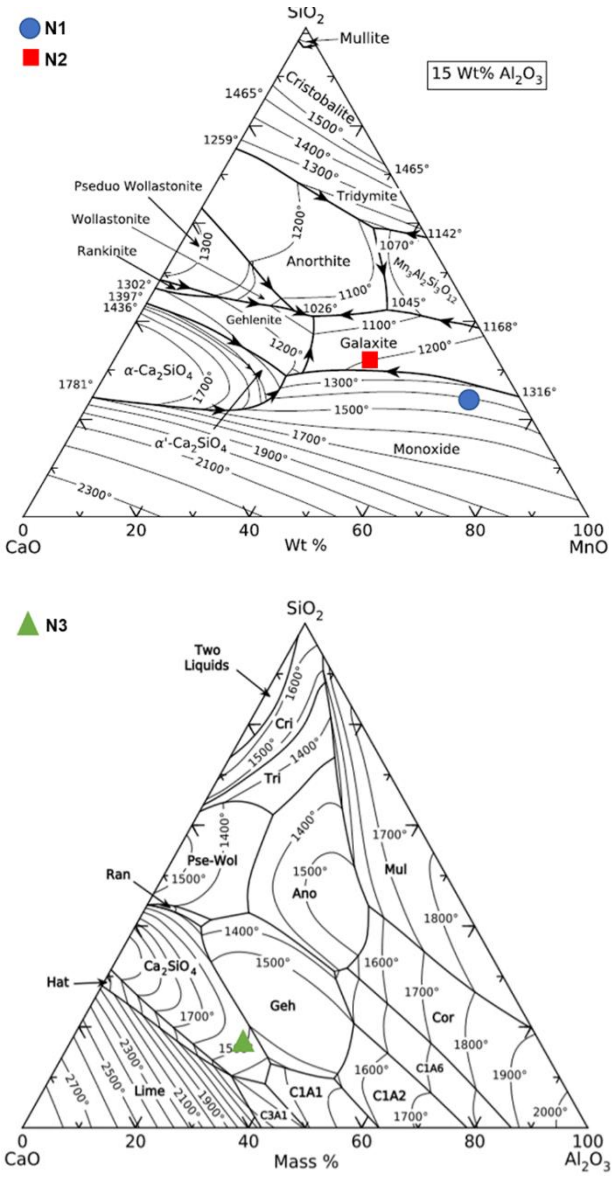

Figure 14: $CaO\text{-}SiO_2\text{-}MnO$ phase diagram[17] (top) and $CaO\text{-}SiO_2\text{-}Al_2O_3$ ternary phase diagram[18] (bottom) used for approximate liquidus temperature of oxide inclusions.

Another important factor could be related to effect of lubricating layer. A lubricating layer was found on all the machine tools during machining of 303 stainless steel. The main component of the lubricating layer comprised of *MnS* inclusions. An additional oxide lubricating layer was found on the *Ca*-treated steels that consisted of *Ca,*

Si, and *Al*. From the SEM images shown in Figure 10 the *Ca*-treated steels appear to have a more stable lubricating layer compared to specimen N1. The thickness of the lubricating layers for the Ca-treated steels were thicker than that of the base steel. Helle[16] studied the interactions of inclusions in steel and cutting tools and found that the presence of oxide inclusions can form a more stable lubricating layer compared to a *MnS* lubricating layer on sintered carbide machine tools. This additional lubricating layer can contribute to a reduction in tool wear during machining.

5. CONCLUSIONS

The machinability of 303 stainless steel was quantified by measuring the progressive flank wear and corresponding tool life. It was found that *Ca*-treatment improves the machinability of 303 stainless steel by increasing the tool life by almost 5 times compared to the untreated steel. *Ca*-treatment affects many factors that can contribute to the improved machinability. *Ca*-treating improves the machinability by modifying the *MnS* inclusions to be more globular which can improve chip formation. The oxide inclusions are also modified by *Ca*-treatment to be more deformable during machining. In addition, a modified oxide lubricating layer was found on the *Ca*-treated steels that can act as an additional lubrication layer and diffusion barrier that may help to stabilize the *MnS* layer to further reduce tool wear during machining.

ACKNOWLEDGEMENTS

The authors would like to thank the industrial sponsors of the Kent D. Peaslee Steel Manufacturing Research Center for funding this research.

REFERENCES

1. Klocke, F., & Kuchle, A. (2013). *Manufacturing Processes 1 Cutting*. Berlin: Springer.

2. Ånmark, N., Karasev, A., & Jönsson, P. (2015). The Effect of Different Non-Metallic Inclusions on the Machinability of Steels. *Materials,8*(2), 751-783. doi:10.3390/ma8020751

3. Kaladhar, M., Subbaiah, K. V., & Rao, C. S. (2012). Machining of austenitic stainless steels - a review. *International Journal of Machining and Machinability of Materials,12*(1/2), 178. doi:10.1504/ijmmm.2012.048564

4. Ånmark, N., Karasev, A., & Jönsson, P. G. (2016). The Influence of Microstructure and Non-Metallic Inclusions on the Machinability of Clean Steels. *Steel Research International,88*(1), 1600111. doi:10.1002/srin.201600111

5. Li, Z., & Wu, D. (2010). Effect of Free-cutting Additives on Machining Characteristics of Austenitic Stainless Steels. *Journal of Materials Science & Technology,26*(9), 839-844. doi:10.1016/s1005-0302(10)60134-x

6. Akasawa, T., Sakurai, H., Nakamura, M., Tanaka, T., & Takano, K. (2003). Effects of free-cutting additives on the machinability of austenitic stainless steels. *Journal of Materials Processing Technology,143-144*, 66-71. doi:10.1016/s0924-0136(03)00321-2

7. Bletton, O., Duet, R., & Pedarre, P. (1990). Influence of oxide nature on the machinability of 316L stainless steels. *Wear,139*(2), 179-193. doi:10.1016/0043-1648(90)90044-b

8. Fang, X., & Zhang, D. (1996). An investigation of adhering layer formation during tool wear progression in turning of free-cutting stainless steel. *Wear,197*(1-2), 169-178. doi:10.1016/0043-1648(96)06924-4

9. M. Harris, O. Adaba, S. Lekakh, R. O'Malley, V. Richards: AISTech Proceedings, 2015, pp. 3315–25.

10. Adaba, Obinna & O'Malley, Ronald & Xu, Mingzhi & Bartlett, Laura & Lekakh, Simon. (2018). Three-Dimensional Study of Inclusion Morphology and Size Distribution In Mn-Si Killed Steel.

11. Kim, S., & Park, Y. (2009). Effects of copper and sulfur additions on machinability behavior of high performance austenitic stainless steel. *Metals and Materials International,15*(2), 221-230. doi:10.1007/s12540-009-0221-6
12. Desaigues, J., Lescalier, C., Bomont-Arzur, A., Dudzinski, D., & Bomont, O. (2016). Experimental study of Built-Up Layer formation during machining of high strength free-cutting steel. *Journal of Materials Processing Technology,236*, 204-215

13. Qi, H., & Mills, B. (1996). On the formation mechanism of adherent layers on a cutting tool. *Wear,198*(1-2), 192-196. doi:10.1016/0043-1648(96)80023-8

14. Harju, E., Kivivuori, S., & Korhonen, A. (1999). Formation of a wear resistant non-metallic protective layer on PVD-coated cutting and forming tools. *Surface and Coatings Technology,112*(1-3), 98-102. doi:10.1016/s0257-8972(98)00771-3

15. Laizhu, J., Kun, C., & Hänninen, H. (1996). Effects of the composition, shape factor and area fraction of sulfide inclusions on the machinability of re-sulfurized free-machining steel. *Journal of Materials Processing Technology,58*(2-3), 160-165. doi:10.1016/0924-0136(95)02144-2

16. A.S. Helle, "ON THE INTERACTION BETWEEN INCLUSIONS IN STEEL AND THE CUTTING-TOOL DURING MACHINING", *Acta polytechnica Scandinavica. Ch, Chemical technology and metallurgy series*, (228), 1995, pp. 2-85

17. Y. B. Kang, I. H. Jung, S. A. Degterov, A. D. Pelton, and H. G. Lee, ISIJ Int., 44 [6] 975-983

18. H. Mao, M. Hiller, M. Selleby, and B. Sundman, J. Am. Ceram. Soc., 89 [1] 298-308 (2006)

SECTION

4. CONCLUSION

The effect of different non-metallic inclusions on the machinability of four different industrially produced steels was investigated. A SEM/EDX was used to characterize the non-metallic inclusions present in the steel. There are numerous effects that inclusions can have on the machinability of steel. In the case of the 4140 steel surrounding the oxide inclusions by sulfide shells can reduce the abrasive nature of the oxide inclusions. This can lead to a decrease in tool wear. This also allowed the Al-rich oxide cores and Ca-Al encapsulated inclusions plastically deform during machining assisting chip formation. There was also evidence of Mn, S, Ca, and Si on the rake surface of the machine tool suggesting the presence of a lubricating layer. In the case of the AR450 steel the number of inclusions per unit area had a significant impact on the final flank wear during the fixed volume machining tests. It was shown that too few inclusions present in the steel, chip formation is difficult which has a detrimental effect on machinability. On the other hand, too many abrasive inclusions per unit area can also have a negative impact on the machinability. Modification of inclusions by Ca-treatment can improve the machinability of resulfurized 303 stainless steel. It was shown that Ca-treatment can modify the oxide inclusions to form lower melting point oxides close to the gehlenite phase field that can be heavily deformed during machining. These oxides can assist in chip formation. The MnS inclusions in the Ca-treated steels also show the possibility to be globularized, and promote a higher density of inclusions which could influence the machinability.

The oxide inclusions promoted by Ca-treatment seemed to stabilize the lubricating layer during machining. In the case of the treated super austenitic stainless steel the synergistic effects of grain size and non-metallic inclusions were investigated. It was found that the treated steel had a 13% decrease in flank wear when compared to the base steel.

5. FUTURE WORK

5.1. CHARATERIZATION OF GRAIN-PINNING PRECIPITATES

The AISI 4140 steel studied has vanadium and aluminum additions to the steel for the purpose of grain pinning during heat treatment. Aluminum will be in the form of AlN precipitates, while vanadium would be present as VN or V(C,N) for grain pinning applications. These precipitates are sub-micron in size, and a transmission electron microscopy (TEM) investigation would be necessary to observe the presence of these precipitates. The results could show some differences in the precipitate properties, and this may influence machinability.

5.2. IMPROVEMENT OF CACLIUM TREATMENT FOR ENHANCED MACHIANBILITY OF 303 STAINLESS STEEL

The calcium treated grades of 303 stainless steel N2 and N3 showed a significant increase in tool-life compared to the base grade of 303 stainless steel. This was the result of modifying the oxide inclusions to be deformable in the primary shear zone to assist chip formation, and promote a more stable lubricating layer on the machine tool. The modified oxide inclusions were nearing the targeted region of the $CaO\text{-}SiO_2\text{-}Al_2O_3$ ternary phase diagram, but further modification of the oxide inclusions can greatly increase the tool-life. From the literature review anorthite inclusions show the greatest benefit to machinability due to the lower melting temperature of this oxide inclusion. Gehlenite oxides are also favorable for increasing machinability, but to a lesser extent.

It would be beneficial to carry out a thermodynamic study of modifying the oxide inclusions to determine the optimal conditions during calcium treatment and other additions to target the formation of anorthite oxide inclusions. This could then be coupled

with sampling of the non-metallic inclusions with SEM/EDX of industrial heats to further improve the machinability of 303 stainless steel.

5.3. EFFECT OF EQUIAXED GRAIN SIZE ON MACHINABILITY

Grain refinement of the cast structure of austenitic stainless steels are of great importance. Equiaxed grains are targeted for better material performance. In this work a finer columnar grain size was achieved in super austenitic stainless steel, which had an improvement of the machinability. A new experimental heat with a fully refined equiaxed structure would be beneficial to investigate the effect of fine equiaxed grains on machinability.

Investigating the individual effects of grain size and non-metallic inclusions separately would be beneficial. Conducting an experimental heat while casting a base steel, and a steel inoculated with TiN and Al_2MgO_4 inclusions poured at a high pouring temperature to influence a similar columnar structure in both steels to look at the effect of the abrasive inclusions on machinability testing. One way to study the grain size of the castings would be to vary the amount of superheat during the pour. When identifying the effect of grain size on machinability two castings could be poured, one with a very low superheat to promote an equiaxed grain structure, and the other casting with a much higher amount of superheat to promote a columnar structure.

APPENDIX A.

EXCERPT OF WORK COMPLETED BY MARK EMMENDORFER FOR EFFECT OF GRAIN REFINING ON PROPERTIES OF SUPERAUSTENITIC STAINLESS STEEL

EFFECT OF GRAIN REFINING ON PROPERTIES OF SUPERAUSTENITIC STAINLESS STEEL

Dustin A. Arvola, Mark C. Emmendorfer, Ronald J. O'Malley, Simon N. Lekakh, Laura N. Bartlett

Missouri University of Science and Technology
Materials Science & Engineering Dept.
1400 N Bishop, Rolla, MO, U.S.A., 65409
Phone: (260) 435-9750
Email: lekakhs@mst.edu

Keywords: superaustenitic stainless steel, grain refinement, segregation, mechanical properties, machinability, corrosion resistance

ABSTRACT

A grain refined structure in high alloy *19Cr-17Ni-6Mo* superaustenitic stainless steel was achieved by the *in-situ* formation of titanium nitrides (*TiN*) on previously formed spinel ($MgAl_2O_4$) inclusions, thus promoting heterogeneous nucleation of austenite during solidification. The alloys were cast under laboratory conditions in a sand mold, producing a heavy section 100 lb. cylindrical casting. These castings were subjected to a homogenization heat treatment based on industry practice for superaustenitic steel, and no coarsening or additional refining of the as-cast grain structure was observed in either the base or grain refined steels. An automated ASPEX SEM/EDX analysis was used to analyze non-metallic inclusions and interdendritic *Cr*, *Ni*, and *Mo* segregation. It was found that the grain refined structure was more effective at reducing interdendritic segregation after heat treatment than the unmodified steel. The

experimentally measured segregation was compared to predicted results using a scheil solidification model.

The properties of an unmodified and inoculated steel were compared in this work. Tensile testing in the heat-treated condition revealed improvements in ultimate tensile strength, ductility, and yield strength for the grain refined material. The room temperature impact properties exhibited a slight decrease in average impact energy, but showed reduced variability compared to the base steel. Fixed volume machining tests were conducted for material in the base and inoculated condition. The machining results showed that the inoculated steel had a slightly improved machinability. This appears to be due to the finer grain size of the modified steel which may offset the potential negative impact of the higher volume fraction of non-metallic inclusions in the grain refined steel. Corrosion testing was performed at an elevated temperature (ASTM A262-15 Practice B) and at room temperature (ASTM G48-11 Method A) to determine corrosion rate and pitting characteristics. The inoculated alloy compared to the base alloy exhibited a decrease in corrosion rate, but an increase in mass loss due to pitting. Characterization of base *vs* inoculated high alloy superaustenitic stainless steel reveals the merits of using inoculation during the steelmaking process to improve the properties of cast products.

1. INTRODUCTION

In addition to the verification of the effect of grain refinement on mechanical properties and corrosion resistance, the impact of grain refinement on machinability were also evaluated. The definition of machinability is the ease with which a material can be machined. This can be evaluated by several parameters: tool life, tool forces, surface roughness of the workpiece, and chip formation.[15] The tool life criterion is one of the

more common practices of defining the machinability of a material.[16] Superaustenitic stainless steel is known to be very difficult to machine. This is because of the high alloying content namely *Cr*, *Ni*, and *Mo*. Problems associated with machining this kind of stainless steel include: excessive tool wear in the forms of flank wear, notch wear, crater wear, edge chipping, and built-up edge.[17-19] It is more common to find research on the machinability of 304 and 316 austenitic stainless steel; however, there is little research done on the machinability of superaustenitic stainless steel. Previous research has investigated the effect of grain size on the machinability of 304 stainless steel. Komatsu et al. studied the effect of grain size during micro-milling.[20] They found that when the grain size was decreased from 9 μm to 1.5 μm the surface finish was significantly improved by reduction of burr formation during machining. Jiang et al. studied the effect of grain size on the tool life during machining of 304L.[21] They varied the grain size by varying the holding temperature after hot-working to promote grain growth. Tool wear increased as grain size increased. Many researchers studied the effect of abrasive inclusions on machinability of different steels.[22-26] Their findings agree that tool life is decreased when machining a steel with a higher volume fraction of inclusions compared to machining a cleaner steel. No research was found that investigated the combined effects of grain size reduction and the presence of abrasive inclusions on machinability of a steel.

2. EXPERIMENTAL PROCEDURE

2.1. Cast steels and sampling

Two pairs of experimental heats were conducted in a 100 lb. coreless induction furnace and details of inoculation treatment for grain refinement were described

elsewhere.[7] The charge material used in all heats were ingots possessing the desired base composition of the targeted superaustenitic stainless steel alloy. These ingots were melted under an argon cover. A set of two unmodified (base) heats underwent a deoxidizing treatment by adding aluminum and calcium wire to the tap stream during furnace tap into the ladle. The furnace was tapped at a temperature of 1640 ^{o}C. The melt was then poured at a temperature of 1500 ^{o}C into a no-bake, silica sand mold shown in Figure 1(a) thus producing a cylindrical casting with a 100 mm diameter. The melt treatment in Figure 1(b) indicates the steps of the casting process in the pair of inoculated heats which targeted grain refinement. The melt was deoxidized with aluminum, calcium treated, and argon stirred. Nitrogen content of the melt was adjusted by an addition of nitrided ferrochrome in the furnace just before tapping into the ladle at a temperature of 1640 ^{o}C. Nuclei forming additions of *Mg-Al-Ti* were made in the ladle just prior to pouring into the mold at 1500 ^{o}C. One casting from each set (base and refined) was used to study microstructure and mechanical properties while the remaining two castings from each set were used for the machinability tests

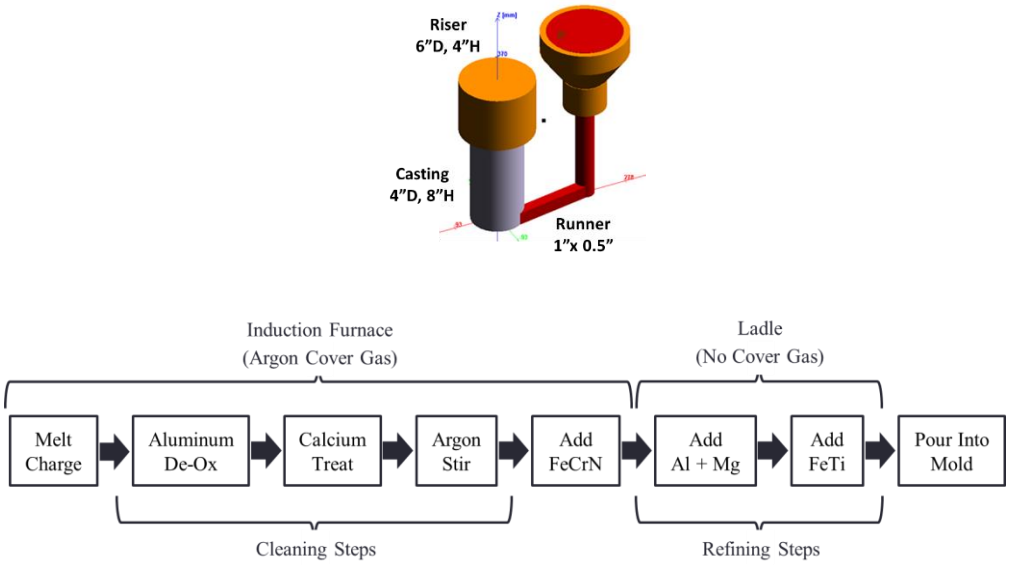

Figure 1. Mold design (top) and a layout of the grain refining melt treatment (bottom) used in this study.

An outline of the composition achieved in both heats are outlined in Table 1. These values were collected by spectrometer and LECO combustion analyzer. The biggest difference in heat design can be observed in the quantity of nuclei forming elements *Mg-Al-Ti-N*.

Table 1. Chemistries of experimental heats, wt.%.

Heat	**Base Elements**							**Nuclei Formers**			
	C	***Si***	***Mn***	***Cr***	***Mo***	***Ni***	***Cu***	***Mg***	***Al***	***Ti***	***N***
Base	0.03	0.63	0.54	19.2	6.08	17.1	0.64	0.000	0.01	0.00	0.093
Refined	0.04	0.78	0.54	18.9	5.92	17.4	0.65	0.009	0.08	0.07	0.091

2.2 Characterization of properties

Machining test specimens were prepared according to the schematic shown in Figure 5. The second heat in each casting set were carried out specifically to produce large specimens for the comprehensive machinability study. The chemistry of the heats are similar to those shown in Table 1. These castings were also heat treated accordingly to the heat schedule outlined in section 2.1. The as-cast surface layer was removed prior to starting each test. A live center was also used to increase the rigidity during machining. The machining tests were carried out on a HAAS TL-1 CNC lathe. The machining parameters were chosen for this study: cutting velocity 53 m/min, depth of cut 0.81 mm, feed rate 0.13 mm/rev, and dry cutting condition. A Sandvik Coromant SNMG 431 QM-235 coated cemented carbide tool was used for this study. Two fixed volume machining tests were completed for each condition to test the repeatability of the machining conditions. The test was completed after machining about 309 cm^3 of material. The progressive flank wear was measured throughout the test, and the final flank wear was recorded. The material with the lower final flank wear exhibited better machinability. Because material was removed during machining, the only qualitative observation of the real macro structure was done visually on fine machined surface each time after several machining steps.

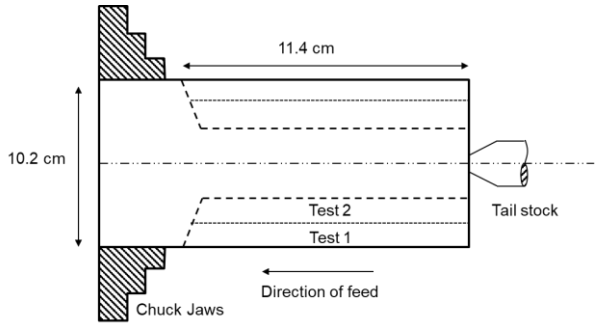

Figure 4. Machining test specimen.

Machine chips were collected and analyzed in a SEM to determine the influence of non-metallic inclusions on chip formation. The worn surfaces of the cutting tools were also investigated. These analyses were completed to determine the synergistic effects of non-metallic inclusions and grain size on machinability of super austenitic stainless steel.

3. RESULTS & DISCUSSION

3.1. Effect of grain refinement on properties

Machining. Heavy section castings from superaustenitic steel were subjected to intensive machining. The effect of grain refinement on machinability was verified on the second set of experimental castings. The average grain size was qualitatively estimated during machining for the top, middle, and bottom position of cut section in the base and inoculated castings, and are shown in Table 5. The casting from the base steel has a significantly coarser grain size overall when compared to the refined casting. The refined casting has a finer grain size due to the addition of active nuclei in the melting process. For example, the top section the base casting has a grain size of 8.0 mm while the refined casting has a grain size of 2.9 mm; however, in studied heavy section casting, the grain size near the chilled bottom are similar in both conditions.

Table 5. Average grain size for the unmodified and modified steels.

Parameter	**Base**			**Refined**		
	Bottom	Middle	Top	Bottom	Middle	Top
Average grain size, mm	3.3	6.6	8.0	2.7	4.7	2.9

The progressive flank wear measurements from the machining tests can be seen in Figure 13. The refined castings had a final flank wear value of 0.188 mm, although the base castings had a final flank value of around 0.21 mm after machining an equivalent volume of material. The second test showed good repeatability of measured flank wear. This results in a 13% decrease in flank wear for the refined casting when machining under the same cutting conditions, and giving the refined castings a slightly improved machinability.

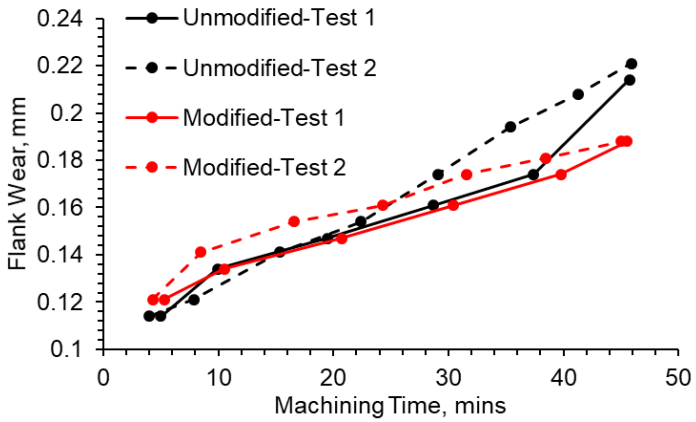

Figure 13. Progressive flank wear curves for the base and refined steels. The machining parameters were chosen for this study: cutting velocity 53 m/min, depth of cut 0.81 mm, feed rate 0.13 mm/rev, and dry cutting condition.

There are several factors that could affect the machinability in grain refined steels including grain size, segregations and non-metallic inclusions. A decrease in grain size and segregations was observed for the refined alloy using *TiN* and *Al-Mg* spinel inclusions. The inclusions present in the base casting are complex oxides containing *Mn-Al-Ti* and some *MnS* inclusions. Overall, the inclusion populations are consistent throughout the machining volume when comparing the top and the bottom locations. However, the inclusion population density was nearly 4 times larger in the refined alloy.

Jiang, et al. varied the grain size of a 304 stainless steel by hot working, and observed that the finer grain size specimens exhibited better machinability.[21] Holappa et al. reported a clean steel will have a detrimental effect on machinability.[22] Multiple authors show that the presence of abrasive oxide inclusions in different steels will lead to an increase in tool wear, and that a higher volume fraction of abrasive inclusions decrease tool life.[23-25] From these reported results it seems that the presence of specific types of inclusions can be beneficial for machinability, but too many abrasive inclusions can lead to aggressive tool wear. No previous studies investigate the combined effects of non-metallic inclusions and grain size. The benefit of the finer grain size of the modified steel offsets the negative effect of abrasive non-metallic inclusions present in the steel.

The cutting tools used in both steels showed built-up edge, flank wear, some chipping wear, and excessive notch wear. The rake surface of the worn cutting tools shown in Figure 14 was investigated. Figures 14(a,b) are the surfaces of the cutting tools for the base and refined steels respectively. A noticeable difference in the region of the rake surface that the chips flow over was observed between these two steels. Inclusions present in both the base and refined steels were found in the chip flow region. Table 6

shows the elemental makeup of the inclusions found on the machining tool. The same type of complex oxide found in the case of the base condition. It can also be seen that in the case of the refined condition *TiN* and $MgAl_2O_4$ spinel inclusions were observed on the cutting tool.

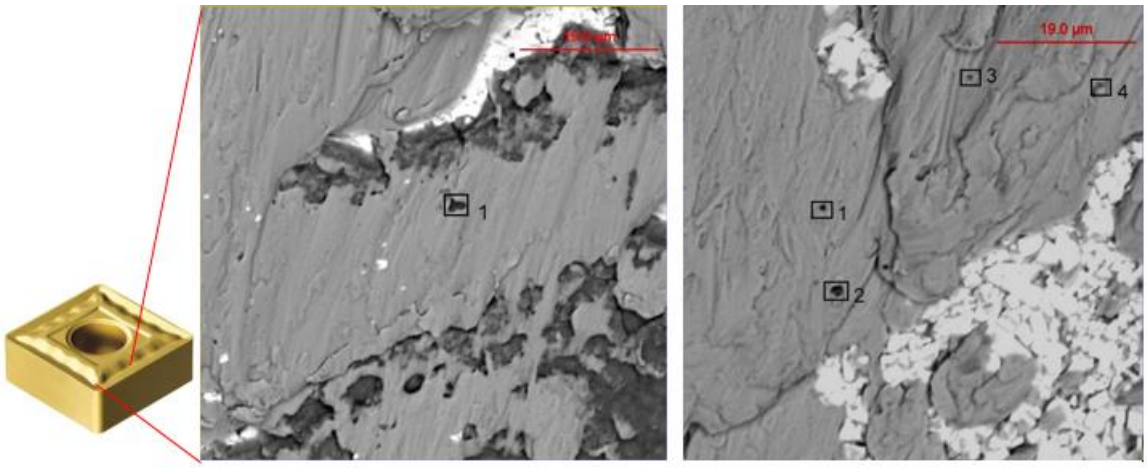

(a) (b)

Figure 14. The SEM image of rake surface of the cutting tool used for machining the base steel (a) and the refined steel (b). The chemical composition of the inclusions observed on the rake surface are listed in the table below.

Table 6. EDX Results of the Inclusions Found on the Rake Surface of the Cutting Tool

Steel	**Area**	***Cr***	***Mn***	***N***	***Ti***	***Al***	***Mg***
Base	1	47.3	39.7	-	6.7	6.3	-
Refined	1	-	-	-	-	79.7	20.3
	2	-	-	-	-	77.5	22.5
	3	-	-	22.2	77.8	-	-
	4	-	-	30.2	66.7	-	-

Machine chips for both base and refined conditions were also observed in SEM. The serrated type of chips shown in Figure 15(a) were formed under the machining conditions

for both steels. Higher magnification of the SEM images in Figure 15(b,c) show a region of the machine chip from the refined steel that was heavily deformed during machining. The EDX results from points 1, 2, and 3 can be seen in Table 7**.** Area 1 is the matrix which consists of *Fe, Cr, Ni,* and *Mo*. Area 2 is a fractured *TiN* inclusion, and the other voids above the crack are visible in Figure 15(c) which showed signals of fractured *TiN* inclusions. Area 3 is a second phase that is rich in *Cr* and *Mo,* but lean in *Ni* this is evident of the σ-phase found in high alloyed stainless steels. This phase is obviously brittle due to it being fractured in multiple areas.[9] Both steels have σ-phase present in the steel, which can weaken the matrix material during machining. The refined steel has a higher volume fraction of inclusions which fractured during machining. This could lead to a lower force required for machining. Zanatta et al. found fractured *Ti(C,N)* inclusions in their chip analysis when machining VP100 mold steel.[26] They measured cutting forces during machining and showed a decrease in cutting forces when machining steel with elevated *Ti* content, in the form of *Ti(C,N)* inclusions. They claimed this could be due to the fracture of the inclusions during machining. Singh et al. also observed a decrease in tool forces during machining a steel with a higher volume fraction of hard inclusions.[24] However, both studies show an increase in flank wear when machining steels with a higher volume fraction of hard inclusions. The lower flank wear reported in this study could be due to the finer grain size of the modified steel which balances the negative effect of the higher volume fraction of *TiN* inclusions.

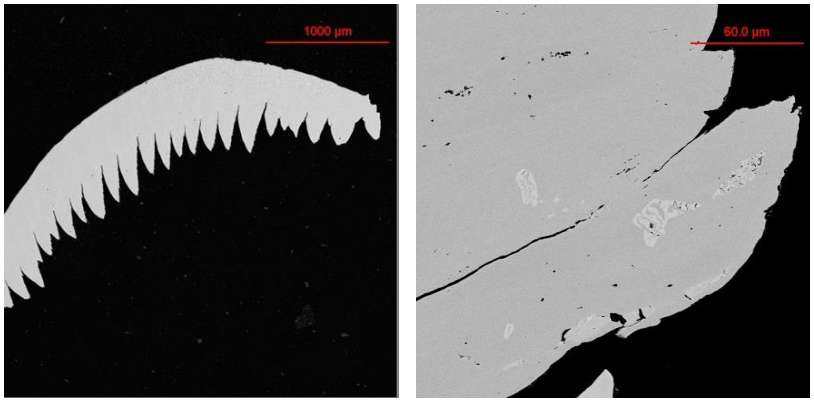

(a) (b)

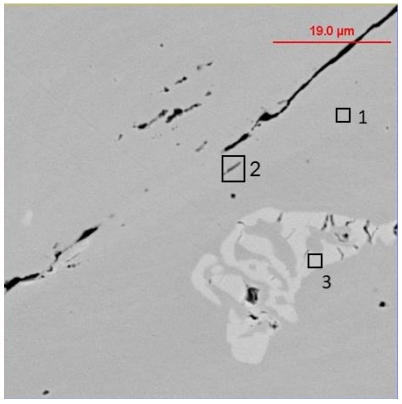

(c)

Figure 15. SEM image of a representative machine chip collected during machining (a) (both steels had serrated chips present in machining), (b) and (c) are higher magnification SEM images of a machine chip showing fractured σ-phase and *TiN* inclusions. The EDX results of the points in (c) can be seen in the table below.

Table 7. EDX analysis (wt.%) of the points shown in Figure 15(c).

Area	*Fe*	*Cr*	*Ni*	*Mo*	*Ti*
1	53.2	22.7	18	4.8	
2	42.8	18.1	15.1	4	18
3	50.2	27.3	11.4	9.3	

4. CONCLUSIONS

The refined steel exhibited slightly improved machinability by decreasing the final flank wear by 13% for the fixed volume of machined material when compared to the base steel. The fine grain size offset the negative effect of inclusions present in the modified steel when compared to the unmodified condition. Mass losses due to pitting corrosion were nearly four times larger for the refined alloy than the base alloy. These pits were caused by the dissolving of clustered *TiN* and spinel inclusions in ferric chloride solution. However, the refined alloy experienced a 30% decrease in corrosion rate during intergranular corrosion testing. This improvement may be related to the improved homogenization of the segregated regions.

5. REFERENCES

1. F. Klocke, A. Kuchle, Manufacturing Processes 1 Cutting, *Springer*, 2013.
2. N. Ånmark, A. Karasev, P. Jönsson, *Materials*, 2015, 8(2), pp. 751-83.
3. M. Alabdullah, A. Polishetty, J. Nomani, G. Littelfair, *Int. J. Adv. Manuf. Tech.*, 2016, 91(1-4), pp. 501-16.
4. M. Alabdullah, A. Polishetty, J. Nomani, *Materwiss Werksttech*, 2017, 48(3-4), pp. 190-197.
5. Polishetty, M. Alabdullah, G. Littelfair, *MATEC Web of Conferences*, 2017, 95.
6. T. Komatsu, T. Yoshino, T. Matsumura, S. Torizuka, *Procedia CIRP*, 2012, 1, pp. 150-55.
7. L. Jiang, Å. Roos, P. Liu, *Metall. Mater. Trans A*, 1997, 28(11), pp. 2415-22.
8. L. Holappa, A. Helle, *J. Mater. Process. Technol.*, 1995, 53(1-2), pp. 177-86.
9. Z. Hong, X. Wu, C. Kun, *Steel Research*, 1995, 66(2), pp. 72-76.
10. S. Singh, A. Chakrabarti, A. Chattopadhyay, *J. Mater. Process. Technol.*, 1997, 66(1-3), pp. 90-96.
11. G. Faulring, S. Ramalingam, *Metall. Trans. A*, 1979, 10(11), pp. 1781-88.
12. Zanatta, J. Gomes, J. Bressan, C. Barbosa, *Adv. Mater. Res.*, 2011, 223, pp. 464-72.
13. M. Harris et al., *AISTech Proceedings*, 2015, pp. 3315–25.

APPENDIX B.

COPYRIGHT INFORMATION FOR PUBLISHED PAPERS

Permission was granted from MS&T 2018 conference proceedings to include Paper I and Paper II in this thesis. They request this thesis to be published after October 18, 2018 after the proceedings have been published. Any author requesting to use Paper I or Paper II needs to include the citation from the MS&T 2018 conference proceedings.

REFERENCES

1. Klocke, F., & Kuchle, A. (2013). *Manufacturing Processes 1 Cutting*. Berlin: Springer.

2. Ånmark, N., Karasev, A., & Jönsson, P. (2015). The Effect of Different Non-Metallic Inclusions on the Machinability of Steels. *Materials,8*(2), 751-783. doi:10.3390/ma8020751

3. Rózański, P & Paduch, J. (2003). Modification of non-metallic inclusions in steels with enhanced machinability. Archives of Metallurgy. 48. 285-307

4. ISO 3685:1993. Tool-life testing with single point turning tools.

5. Chinchanikar, S., & Choudhury, S. (2013). Investigations on machinability aspects of hardened AISI 4340 steel at different levels of hardness using coated carbide tools. *International Journal of Refractory Metals and Hard Materials,38*, 124-133. doi:10.1016/j.ijrmhm.2013.01.013

6. Kuljanic, Elso, Marco Sortino, and Giovanni Totis. "Machinability of difficult machining materials." *submitted to International Research/Expert Conference Trends in the Development of Machinery and Associated Technology*. 2010.

7. Bletton, O., Duet, R., & Pedarre, P. (1990). Influence of oxide nature on the machinability of 316L stainless steels. *Wear,139*(2), 179-193. doi:10.1016/0043-1648(90)90044-b

8. Kronenberg, M. *Machining Science and Application: Theory and Practice for Operation and Development of Machining Processes*. Pergamon Press, 1966.

9. Desaigues, J., Lescalier, C., Bomont-Arzur, A., Dudzinski, D., & Bomont, O. (2016). Experimental study of Built-Up Layer formation during machining of high strength free-cutting steel. *Journal of Materials Processing Technology,236*, 204-215

10. Fang, X., & Zhang, D. (1996). An investigation of adhering layer formation during tool wear progression in turning of free-cutting stainless steel. *Wear,197*(1-2), 169-178. doi:10.1016/0043-1648(96)06924-4

11. Qi, H., & Mills, B. (1996). On the formation mechanism of adherent layers on a cutting tool. *Wear,198*(1-2), 192-196. doi:10.1016/0043-1648(96)80023-8

12. Trent, E. M. *Metal Cutting*. Butterworths, 1979.

13. Matsumoto, Y., et al. “Cutting Mechanism during Machining of Hardened Steel.” *Materials Science and Technology*, vol. 3, no. 4, 1987, pp. 299–305., doi:10.1179/mst.1987.3.4.299.

14. Shelbourn, A. M., et al. “Structures of Machined Steel Chips.” *Materials Science and Technology*, vol. 1, no. 3, 1985, pp. 220–226., doi:10.1179/mst.1985.1.3.220.

15. Wright, P. K., and J. L. Robinson. “Material Behaviour in Deformation Zones of Machining Operation.” *Metals Technology*, vol. 4, no. 1, 1977, pp. 240–248., doi:10.1179/030716977803292042

16. Davim, J. Paulo. *Machining: Fundamentals and Recent Advances*. 2010.

17. Faulring, G. M., & Ramalingam, S. (1979). Oxide inclusions and tool wear in machining. *Metallurgical Transactions A,10*(11), 1781-1788. doi:10.1007/bf02811716

18. Diggs, V. J., et al. “35th Mechanical Working and Steel Processing Conference; 1993; Pittsburgh; PA.” Iron and Steel Society, *MECHANICAL WORKING AND STEEL PROCESSING*, vol. 31, 1994, pp. 131–138.

19. Hamann, J.c., et al. “Machinability Improvement of Steels at High Cutting Speeds – Study of Tool/Work Material Interaction.” *CIRP Annals*, vol. 45, no. 1, 1996, pp. 87–92., doi:10.1016/s0007-8506(07)63022-4.

20. Kaushik, P, et al. “Inclusion Characterisation for Clean Steelmaking and Quality Control.” *Ironmaking & Steelmaking*, vol. 39, no. 4, 2012, pp. 284–300., doi:10.1179/1743281211y.0000000069.

21. Ruppi, S., Hogrelius, B., & Huhtiranta, M. (1998). Wear characteristics of TiC, Ti(C,N), TiN and Al2O3 coatings in the turning of conventional and Ca-treated steels. *International Journal of Refractory Metals and Hard Materials,16*(4-6), 353-368. doi:10.1016/s0263-4368(98)00039-0

22. Laizhu, J., Kun, C., & Hänninen, H. (1996). Effects of the composition, shape factor and area fraction of sulfide inclusions on the machinability of re-sulfurized free-machining steel. *Journal of Materials Processing Technology,58*(2-3), 160-165. doi:10.1016/0924-0136(95)02144-2

23. Yaguchi, Hiroshi. “Effect of MnS Inclusion Size on Machinabilty of Low-Carbon, Leaded, Resulfurized Free-Machining Steel.” *Journal of Applied Metalworking*, vol. 4, no. 3, 1986, pp. 214–225., doi:10.1007/bf02833929.

24. Pytel, S., and S. Rudnik. “Proceedings of the International Conference on Processing, Microstructure, and Properties of Microalloyed and Other Modern High Strength Low Alloy Steel.” *Proceedings of the International Conference on Processing, Microstructure, and Properties of Microalloyed and Other Modern High Strength Low Alloy Steel*, 1992, pp. 13–21.

25. Kiessling, Roland. *Non-Metallic Inclusions in Steel*. Institute of Metals, 1989.

26. Zanatta, A. M., Gomes, J. D., Bressan, J. D., & Barbosa, C. A. (2011). Influence of Hard and Soft Inclusions on the Machinability and Polishability of VP100 Mold Steel. *Advanced Materials Research,223*, 464-472. doi:10.4028/www.scientific.net/amr.223.464

27. Z. Hong, X. Wu, C. Kun, *Steel Research*, 1995, 66(2), pp. 72-76.

28. Liu, Haitao, and Weiqing Chen. “Effect of Total Oxygen Content on the Machinability of Low Carbon Resulfurized Free Cutting Steel.” *Steel Research International*, vol. 83, no. 12, Dec. 2012, pp. 1172–1179., doi:10.1002/srin.201200053

29. A.S. Helle, "ON THE INTERACTION BETWEEN INCLUSIONS IN STEEL AND THE CUTTING-TOOL DURING MACHINING", *Acta polytechnica Scandinavica. Ch, Chemical technology and metallurgy series*, (228), 1995, pp. 2-85

30. Akasawa, T., Sakurai, H., Nakamura, M., Tanaka, T., & Takano, K. (2003). Effects of free-cutting additives on the machinability of austenitic stainless steels. *Journal of Materials Processing Technology,143-144*, 66-71. doi:10.1016/s0924-0136(03)00321-2

31. Bittès, G., Leroy, F., & Auclair, G. (1995). The relationship between inclusionary deposits and the wear of cutting tools. *Journal of Materials Processing Technology,54*(1-4), 88-96. doi:10.1016/0924-0136(95)01925-1

32. Harju, E., Kivivuori, S., & Korhonen, A. (1999). Formation of a wear resistant non-metallic protective layer on PVD-coated cutting and forming tools. *Surface and Coatings Technology,112*(1-3), 98-102. doi:10.1016/s0257-8972(98)00771-3

33. Kurt Tonshoff, Hans & Cassel, Claus. (1993). Effects of non-metallic inclusions in quenched and tempered steel on the wear behavior of cermet cutting tools. 49. 73-78.

34. Matsui, N., & Watari, K. (2006). Wear Reduction of Carbide Tools Observed in Cutting Ca-added Steels for Machine Structural Use. *ISIJ International,46*(11), 1720-1727. doi:10.2355/isijinternational.46.1720

35. Holappa, L., & Helle, A. (1995). Inclusion Control in High-Performance Steels. *Journal of Materials Processing Technology,53*(1-2), 177-186. doi:10.1016/0924-0136(95)01974-j

36. Ånmark, N., Lövquist, S., Vosough, M., & Björk, T. (2015). The Effect of Cleanliness and Micro Hardness on the Machinability of Carburizing Steel Grades Suitable for Automotive Applications. *Steel Research International,87*(4), 403-412. doi:10.1002/srin.201500243

37. Ånmark, Niclas, and Thomas Björk. "Effects of the Composition of Ca-Rich Inclusions on Tool Wear Mechanisms during the Hard-Turning of Steels for Transmission Components." *Wear*, vol. 368-369, 2016, pp. 173–182., doi:10.1016/j.wear.2016.09.016.

38. L. Jiang, Å. Roos, P. Liu, *Metall. Mater. Trans A*, 1997, 28(11), pp. 2415-22.

39. Hoseiny, H., et al. "The Effect of the Martensitic Packet Size on the Machinability of Modified AISI P20 Prehardened Mold Steel." *Journal of Materials Science*, vol. 47, no. 8, 2011, pp. 3613–3620., doi:10.1007/s10853-011-6208-y

40. T. Komatsu, T. Yoshino, T. Matsumura, S. Torizuka, *Procedia CIRP*, 2012, 1, pp. 150-55.

41. M. Harris, O. Adaba, S. Lekakh, R. O'Malley, V. Richards: AISTech Proceedings, 2015, pp. 3315–25.

VITA

Mark Charles Emmendorfer was born in St. Louis, Missouri. He attended Missouri University of Science and Technology, and graduated with his Bachelor's degree in Metallurgical Engineering in 2016. During his undergraduate studies he had multiple internships at various steel foundries. In the summer of 2014 he worked at MetalTek-Carondelet Division in Pevely, Missouri. In the summer for 2015 he worked for Spokane Industries a steel foundry in Spokane, Washington. He was an active member of the American Foundry Society student chapter, and honored to be a Foundry Education Foundation student. He continued his education in Metallurgy at Missouri University of Science and Technology in June 2016 to pursue a Master's degree. Mark started his research on the machinability of steel during the summer of 2016 for the Kent D. Peaslee Steel Manufacturing Research Center. During his time attending graduate school he worked as the teaching assistant for the metals casting lab. In July 2018 he received his MS degree in Metallurgical Engineering from Missouri University of Science and Technology.